Sandia National Laboratories
Waste Isolation Pilot Plant

Analysis Report for AP-100 Task 1:
Development and Application of
Acceptance Criteria for Culebra Transmissivity (T) Fields

(AP-100: Analysis Plan for Calculations of Culebra Flow and Transport:
Compliance Recertification Application)

Task Number 1.3.5.1.2.1

ERMS# 531136

Author: _____Richard L. Beauheim, 6822_____ Date: _9/8/03_

Technical Review: _____Joseph F. Kanney, 6821_____ Date: _9/8/03_

QA Review: _____Mario J. Chavez, 6820_____ Date: _9/?/03_

Management Review: _____David S. Kessel, 6821_____ Date: _9/8/03_

WIPP:1.3.5.1.2.1:PA:QA-L:DPRP1:531035

Contents

Table

Figures

2

1.   Introduction and Objectives

The Waste Isolation Pilot Plant (WIPP) is located in southeastern New Mexico and has been developed by the U.S. Department of Energy (DOE) for the geologic disposal of transuranic (TRU) waste. Containment of TRU waste at the WIPP is regulated by the U.S. Environmental Protection Agency (EPA) according to the regulations set forth in Title 40 of the Code of Federal Regulations, Parts 191 and 194. The DOE demonstrates compliance with the containment requirements in the regulations by means of a performance assessment (PA), which estimates releases from the repository for the regulatory period of 10,000 years after closure.

In October 1996, DOE submitted the Compliance Certification Application (CCA) to the EPA, which included the results of extensive PA analyses and modeling. After an extensive review, the EPA certified in May 1998 that the WIPP met the criteria in the regulations and was approved for disposal of transuranic waste. The first shipment of waste arrived at the site in March 1999.

The results of the PA conducted for the CCA were subsequently summarized in a Sandia National Laboratories (SNL) report (Helton et al., 1998) and in refereed journal articles (Helton and Marietta, 2000).

The DOE is required to submit a Compliance Recertification Application (CRA) every five years after the initial receipt of waste. The recertification applications take into account any information or conditions that have changed since the original certification decision. Accordingly, the DOE is conducting a new PA in support of the CRA.

The EPA requires that 100 different transmissivity (T) fields be used in modeling flow and transport through the Culebra Dolomite Member of the Rustler Formation to capture the uncertainty associated with the modeling. This Analysis Report documents the development and application of acceptance criteria for calibrated transmissivity (T) fields for the Culebra. The 100 accepted T fields will be used in flow and transport calculations for the WIPP CRA performed under AP-100 (Leigh et al., 2003). The activities described in this Analysis Report constitute Task 1 of AP-100.

T fields for the Culebra were created and calibrated under AP-088 (Beauheim, 2002a). Five hundred different but equally probable base (uncalibrated) T fields were created by Holt and Yarbrough (2003) using observed correlations between Culebra T and dissolution of the upper Salado Formation, thickness of overburden above the Culebra, and the presence of halite in the Rustler members immediately above and below the Culebra. McKenna and Hart (2003a) then attempted to calibrate 150 of the base T fields in MODFLOW-2000 v. 1.6 (Harbaugh et al., 2000) with PEST v. 5.5 (Doherty, 2002) controlling the calibration procedure. Four of the 150 fields could not be calibrated at all, leaving 146. Calibration of the T fields entailed adjusting T values throughout the model domain until model-calculated "steady-state" and transient heads match measured values as closely as possible. The measured "steady-state" heads are not actually representative of steady-state conditions, but are rather the heads measured in 35 wells in late 2000 (Beauheim, 2002b). The transient heads comprise the responses observed in 40 wells to seven large-scale (in terms of area of influence) pumping tests conducted between 1985 and 1996 (Beauheim, 2003).

Model calibration is never perfect. Reasons for irreducible differences between modeled and measured heads include:

- Inaccuracies in boundary conditions
- Differences between the actual storativity in various areas of the Culebra and the single value of storativity (1×10^{-5}) used in the MODFLOW model
- Inability of PEST/MODFLOW to change T as abruptly as may occur in reality
- Constraints placed on PEST concerning the maximum allowable change in T

In practice, the calibration procedure employed by McKenna and Hart (2003a) stopped for one of three reasons for each T field:

1. PEST completed the maximum allowed number of iterations (15)
2. PEST was unable to improve the objective function (sum of squared errors of weighted residuals) for three successive iterations
3. the optimization became numerically unstable

Because the calibration procedure did not stop when some objective goodness-of-fit target was achieved, criteria must be established to define what constitutes an acceptable calibration so that 100 "good" T fields can be used in the WIPP CRA calculations. Because the T fields will be used for calculation of radionuclide transport, the travel times calculated in the T fields for a conservative particle released above the center of the WIPP waste panels to reach the WIPP boundary will be used in evaluating acceptance criteria. That is, we will determine the sensitivity of the calculated travel-time distribution to the proposed acceptance criteria to identify those criteria that are important. Once the distribution of travel times shows no (remaining) sensitivity to continued refinement of the criteria applied (e.g., a reduction in some metric below a threshold value), all T fields meeting those criteria will be considered to be acceptably calibrated.

The travel times discussed herein are based on the times obtained by applying the particle-tracking code DTRKMF v. 1.0 (Rudeen, 2003) to the calibrated MODFLOW-2000 flow fields assuming a single-porosity medium with a porosity of 0.16. The MODFLOW modeling is being performed using a 7.75-m thickness for the Culebra, whereas transport calculations will assume that all flow is concentrated in the lower 4.0 m of Culebra. Therefore, the travel times obtained from DTRKMF are scaled by multiplying by the factor 0.516 (4/7.75). These scaled travel times are then consistent with the travel times calculated and reported by Wallace (1996) for the T fields used in the WIPP CCA (U.S. DOE, 1996). These travel times do not, however, represent the actual predicted travel times of solutes, conservative or non-conservative, through the Culebra. Culebra transport modeling treats the Culebra as a double-porosity medium with transport through advective porosity (e.g., fractures) retarded by diffusion into diffusive porosity (e.g., matrix porosity) and by sorption. The travel times presented herein are intended only to allow comparison among T fields.

4

2. Candidate Acceptance Criteria

Four factors have been evaluated for their potential to provide T-field acceptance criteria: the root mean squared error (RMSE) of the modeled fit to the measured steady-state heads, the agreement between the measured and modeled steady-state gradient/heads, the sum of squared weighted residuals (phi), and the agreement between the measured and modeled transient heads. These factors are not totally independent of one another, but are related in ways discussed below.

2.1 RMSE

The RMSE is a measure of how close MODFLOW/PEST came to matching the measured steady-state heads for each T field. The RMSE is defined as:

$$RMSE = \sqrt{\frac{\sum_{i=1}^{n_{obs}} (H_i^{obs} - H_i^{calc})^2}{n_{obs}}} \tag{1}$$

where n_{obs} is the number of head observations and H^{obs} and H^{calc} are the values of the observed and calculated heads, respectively. Previous Culebra T-field calibration exercises (e.g., LaVenue and RamaRao, 1992) achieved RMSE's less than 3 m in most cases when calibration was being performed only to steady-state heads. RMSE's have not previously been reported for steady-state heads in T fields calibrated to transient heads.

2.2 Fit to Steady-State Heads

One measure of how well a T field has matched the steady-state heads can be obtained by simply plotting the measured heads versus the modeled heads. If the measured and modeled heads match exactly, the best-fit straight line through the data will have a slope of one. Exact agreement between measured and modeled heads is not to be expected, so an acceptance criterion on the slope of the best-fit line must be established.

The steady-state heads are important because the transport calculations that will be performed in SECOTP2D rely on the steady-state velocity field provided by MODFLOW. If MODFLOW has not accurately captured the steady-state heads, steady-state gradients and the associated steady-state velocities will be in error. With measured head plotted as the independent variable (x) and calculated head plotted as the dependent variable (y), a slope of the best-fit line less than unity implies that the calculated gradient is less than the measured gradient. Low gradients should lead to excessively long travel times. Therefore, we would like to determine if a threshold value of the steady-state-fit slope exists above which the distribution of travel times is insensitive.

2.3 Phi

Phi values provide an objective way to compare the goodness of fit of different realizations based on established numerical criteria. The establishment of those numerical criteria is not itself, however, a fully objective process. For the Culebra T fields, four interrelated factors contribute to phi:

- Model match to steady-state heads
- Model match to transient heads
- Weight assigned to each measured head value
- Number of transient head observations

Phi is defined as:

$$\phi = \sum_{i=1}^{n_{obs}^{SS}} (W^{SS}(H_i^{obs-SS} - H_i^{calc-SS}))^2 + \sum_{i=1}^{n_{wells}^{Tr}} \sum_{j=1}^{n_{obs}^{Tr}} (W_i^{Tr}(H_j^{obs-Tr} - H_j^{calc-Tr}))^2 \qquad (2)$$

where n_{obs} is the number of head observations, n_{wells} is the number of wells, W is the weight assigned to a group of measurements, H^{obs} and H^{calc} are the values of the observed and calculated heads, respectively, and superscripts SS and Tr refer to steady-state and transient measurements, respectively.

The steady-state heads consist of single measurements made in 35 wells. The transient heads consist of a total of 1332 measurements made in 40 wells during seven pumping tests (three to ten wells monitored per test). For each measurement, the modeled head is subtracted from the measured head to obtain the residual, and the residual is multiplied by a weight assigned to that well for that test. The residual-weight products are then squared and summed to obtain phi, which has units of meters squared.

The total phi can be divided into steady-state and transient components, as shown by the two parts of the right-hand side of (2). The steady-state phi is a weighted, squared, and summed expression of the RMSE given in (1) above and is not, therefore, meaningful to consider when RMSE is already being considered. Only transient phi will be considered in the discussion that follows.

Transient phi values do not constitute a fully objective measure of the goodness of fit of a T field for several reasons. First, the weights assigned to each well's responses could not be defined in a fully objective manner. For the majority of the transient responses, the weight assigned to a well was the inverse of the maximum drawdown observed at that well during the test (McKenna and Hart, 2003a). Thus, a well at which 6 m of drawdown was observed was assigned a weight of 0.167 (1/6), while a well at which 0.6 m of drawdown was observed was assigned a weight of 1.667 (1/0.6). This served to normalize the responses so that the high-drawdown wells did not dominate the objective function. Under this weighting scheme, two tests that are both fit by the model to within 50 percent of the observed drawdown values (implying that T's are within a factor of two of their "correct" values) would be given equal consideration in the calculation of the overall objective function even though one test may have an observed maximum drawdown of 10 meters and the other a maximum observed drawdown of 0.10 meters. Without this weighting, minimization of the objective function would result in disproportionate effort to optimize T in regions of the model where high drawdowns were observed, at the expense of T values in the rest of the model domain. The weights assigned in this manner ranged from 0.052 to 20.19. We also wished to include the observed absence of a response at WQSP-3 to pumping at WQSP-1 and WQSP-2 in the calibration process, so McKenna and Hart (2003a) inserted "measurements" of zero drawdown that were given an arbitrarily high weight of 20 in the

calibration process. Second, the number of measurements made at individual wells during individual tests range from six to 104, and the number of measurements made at all wells during a single test range from 64 to 410. This means that different well responses carry different cumulative weights, and that different tests carry different cumulative weights. Third, some parts of the modeling domain are covered by multiple wells' responses, while other parts of the domain have no transient response data. This means that some parts of the T field are probably calibrated better than other parts.

Thus, transient phi values do not provide an unbiased measure of how well a calibrated T field represents the actual T field. No simple numerical value can be established that represents an average residual of some meaningful value for each transient measurement, such as the RMSE used to evaluate T-field calibration to steady-state heads alone. Nevertheless, the transient phi values do provide an indication of how well a T field met the calibration targets as defined and might be used qualitatively to define acceptable T fields.

2.4   Fit to Transient Heads

Evaluating the model match to transient heads is not as straightforward as for the steady-state heads because the transient match involves both the magnitude and the timing of head changes. The magnitude and timing of a transient response are governed by both the transmissivity and storativity (S) of a system, but S was not included as a calibration parameter during the calibration process. A single S value of 1×10^{-5} (log = -5) was used during T-field calibration. As reported by Beauheim (2003), the apparent storativities obtained from independent analyses of the test responses used for the calibration range from 5.1×10^{-6} (log = -5.29) to 7.3×10^{-5} (log = -4.14). Because the calibration method only allowed PEST to adjust T to try to match the measured heads, it might actually shift T away from the correct value in trying to compensate for an inappropriate value of S. Thus, some allowance needs to be made for how close PEST could actually come to matching the measured responses.

To establish the bounds of what might be considered acceptable matches to the transient heads, we ran a series of well-test simulations using the code nSIGHTS (Roberts, 2002). For base-case parameter values, we used a T of 1×10^{-5} m^2/s and an S of 1×10^{-5}. We simulated pumping in a well for 5, 25, and/or 50 days, and simulated the responses that would be observed in observations wells 1, 2, and/or 3 km away. We also varied T and/or S by approximately a half order of magnitude upward and downward (3×10^{-5} and 3×10^{-6}). The results of these simulations are shown in Appendix A.

Based on the simulations, a set of guidelines was developed to determine if a modeled response matched a measured response within a half order of magnitude uncertainty in T and/or S. The guidelines are structured around the position of the modeled maximum drawdown relative to the measured maximum drawdown on a linear-linear plot of elapsed time on the x-axis and drawdown (increasing upward) on the y-axis. The guidelines are as follows:

- If the modeled peak occurs early and high (relative to the measured peak), S is too low and the maximum modeled drawdown can be up to three times greater than the maximum measured drawdown.

- If the modeled peak occurs early and low, T is too high and the maximum modeled drawdown can be up to two times lower than the maximum measured drawdown.
- If the modeled peak occurs late and high, T is too low and the maximum modeled drawdown can be up to two times higher than the maximum measured drawdown.
- If the modeled peak occurs late and low, S is too high and the maximum modeled drawdown can be up to three times lower than the maximum measured drawdown.
- If the modeled peak occurs at the same time as the measured peak but is high, the diffusivity (T/S) is correct, but both values are too low and the maximum modeled drawdown can be up to three times greater than the maximum measured drawdown.
- If the modeled peak occurs at the same time as the measured peak but is low, the diffusivity (T/S) is correct, but both values are too high and the maximum modeled drawdown can be up to three times lower than the maximum measured drawdown.

No quantitative criteria were established for how much earlier or later modeled peaks could occur relative to measured peaks because of the wide range observed in the simple scoping calculations shown in Appendix A (calculated peaks occurring a factor of five sooner to a factor of ten later than the observed peaks) and because of the variability in pumping durations and distances to observation wells associated with the measured responses.

Using these guidelines, plots of each of the 40 transient well responses of each calibrated T field can be evaluated visually to determine if the T field represents that response within a half order of magnitude uncertainty in T and/or S. A threshold number of well responses that fail this test can then be considered as a possible acceptance criterion for the T fields.

3. Application of Criteria to T Fields

The four criteria described above must be applied to actual T fields to determine if they allow meaningful discrimination among the fields. Given that travel time is the performance measure of most concern, the four criteria will be evaluated in terms of their effects on the calculated distribution of travel times from the T fields. A total of 146 T fields are available for this evaluation (McKenna and Hart, 2003a).

The measured and modeled heads for the T fields, along with residuals, weights, and other information, are provided in the PEST residuals output files from McKenna and Hart (2003a) designated *d##r##_transient.res*, where the d##r## values correspond to the base T-field designations provided by Holt and Yarbrough (2003). These files are entered into an Excel spreadsheet template and given the designation *d##r##.xls*. RMSE values, phi values, and other values described below are calculated within the Excel spreadsheets. The information is then summarized for all T fields in Table 1 and spreadsheet *Tfield_stats.xls*.

3.1 RMSE

Steady-state RMSE values for all the completed T fields are calculated in cell Y28 in the *d##r##.xls* files, tabulated in column D in file *Tfield_stats.xls*, and plotted in Figure 1. The data for H-9b, the southernmost well, were excluded from the RMSE calculation because the southern model boundary condition consistently caused the modeled H-9b head to be significantly lower than the measured head, disproportionately affecting the calculation of the RMSE. The exclusion of the H-9b data should provide a better measure of the accuracy of the model in the rest of the model domain.
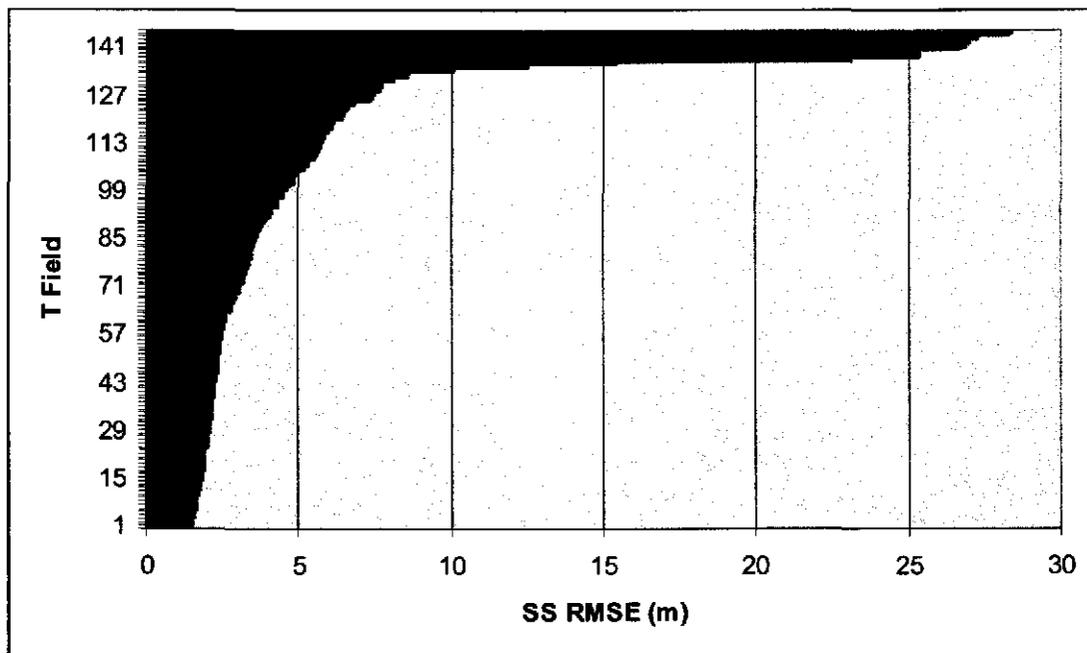

Figure 1.   Steady-state RMSE values for 146 T fields.

Information Only

9

Table 1. Summary information on T fields.

T Field	SS RMSE (m)	SS Phi (m^2)	Transient Phi (m^2)	Steady-State-Fit Slope	# of Failed Well Responses	Time to WIPP boundary (yr)
d01r01	7.427	10498	5486	0.411	13	67578
d01r02	3.915	3621	5110	0.862	20	12045
d01r04	2.812	2140	2563	1.204	11	13821
d01r05	7.313	10245	12643	0.245	16	18886
d01r06	4.856	5006	11426	0.759	15	241211
d01r07	3.377	2851	3187	0.889	9	42123
d01r08	5.484	6122	4091	1.407	14	4399
d01r10	1.646	1094	1476	0.943	9	20685
d02r01	26.966	128711	12359	0.075	19	141516
d02r02	3.507	2772	2889	0.748	11	17217
d02r03	10.070	18606	8173	0.165	15	279242
d02r04	8.104	12482	5305	0.158	12	92235
d02r05	5.184	5577	7224	0.614	17	17255
d02r06	25.325	113652	7810	0.071	16	169677
d02r07	3.648	3223	10047	0.963	15	32231
d02r08	5.001	5125	7713	0.643	17	23571
d02r10	6.066	6849	5312	0.785	13	6433
d03r01	4.506	4022	6053	0.625	17	18435
d03r02	28.346	142152	15357	0.056	16	398937
d03r03	4.146	3899	7102	1.016	17	7171
d03r04	25.367	114006	11991	0.114	14	132833
d03r05	5.836	6873	4585	0.605	13	6638
d03r06	1.729	1208	1899	0.959	13	27006
d03r07	4.655	4740	4399	1.138	13	22599
d03r08	4.550	4250	5593	0.638	17	13942
d03r09	2.352	1574	1580	0.877	7	25757
d03r10	8.584	13811	2766	1.060	13	15054
d04r01	3.447	2370	4736	0.673	17	80690
d04r02	3.818	3175	2647	0.736	12	40593
d04r03	2.352	1659	3317	0.979	12	13888
d04r04	4.298	3692	2697	0.602	13	36245
d04r05	1.507	1059	1980	0.984	9	48168
d04r06	3.705	3146	5618	0.961	16	26199
d04r07	2.183	1397	2226	0.860	10	23105
d04r08	2.444	1759	1560	0.890	11	30470
d04r09	27.256	131491	18356	0.064	16	114087
d04r10	3.060	2401	2593	0.853	9	25316
d05r01	6.427	8119	2015	0.886	13	86924
d05r02	5.298	5831	6755	0.872	16	25610
d05r03	3.444	2580	2655	0.799	11	10880
d05r04	5.862	6984	10518	0.497	17	14856
d05r05	4.346	4226	18478	0.952	16	5668
d05r06	6.518	8198	3609	0.360	13	96589
d05r07	3.188	2682	5216	0.899	9	13766
d05r08	7.686	11242	11194	0.147	16	70896
d05r09	26.644	125685	10840	0.081	17	152818
d05r10	5.623	6497	7110	0.497	16	30955
d06r01	6.828	9057	6592	0.338	17	103442
d06r02	1.957	1266	2639	0.993	9	10353
d06r03	1.637	1051	1703	0.974	10	81258
d06r04	3.214	2246	2805	0.727	13	18294

T Field	SS RMSE (m)	SS Phi (m^2)	Transient Phi (m^2)	Steady-State-Fit Slope	# of Failed Well Responses	Time to WIPP boundary (yr)
d06r05	3.886	3516	5164	0.718	18	36644
d06r06	2.149	1254	2954	1.013	10	14935
d06r07	1.518	784	965	0.951	7	12035
d06r08	7.440	10397	4518	0.343	18	74565
d06r09	28.309	141764	7864	0.046	18	168281
d06r10	2.196	1455	1801	0.876	11	21990
d07r01	3.101	2326	2905	0.811	14	5082
d07r02	2.010	1327	3271	0.934	15	45647
d07r03	15.470	42986	12795	0.320	19	12919
d07r04	5.579	6230	7033	0.699	18	5638
d07r05	2.727	1705	5942	0.958	10	15097
d07r06	4.334	3927	6345	0.540	12	24641
d07r07	2.477	1737	2225	0.908	9	17038
d07r08	2.232	1097	2836	0.843	9	4355
d07r09	2.207	1239	1628	0.909	8	68629
d07r10	1.782	839	1150	0.940	9	15680
d08r01	2.361	1736	2458	0.913	11	4388
d08r02	2.418	1168	1326	0.904	6	26115
d08r03	2.137	1489	1499	0.938	9	28570
d08r04	3.683	2674	2966	0.779	9	24773
d08r05	2.115	1384	2769	0.899	13	15358
d08r06	1.916	1388	1225	0.931	11	13917
d08r07	1.857	815	1333	1.029	10	15027
d08r08	12.534	28547	6267	0.244	12	13885
d08r09	5.785	6674	7437	0.809	17	9691
d09r01	8.621	13909	7050	0.074	11	291623
d09r02	3.243	2418	4482	0.817	12	20048
d09r03	2.252	1337	989	0.937	8	40948
d09r04	1.892	710	1123	0.952	8	12857
d09r05	2.061	954	1088	0.919	8	10726
d09r06	2.794	2313	2253	0.879	16	10509
d09r07	2.629	1676	4591	0.981	10	9472
d09r08	1.895	1030	1406	0.946	9	17741
d09r09	4.826	4945	4453	0.660	14	4359
d09r10	3.273	2790	3976	0.941	19	50791
d10r01	26.867	127794	6006	0.031	14	297840
d10r02	1.554	589	1330	0.967	8	3111
d10r03	2.201	1474	1626	0.955	9	12533
d10r04	2.527	1788	2334	1.097	9	3799
d10r05	5.722	6646	6463	0.460	18	28390
d10r06	4.702	4644	4412	0.702	13	9210
d10r07	1.870	810	1937	0.935	10	10068
d10r08	2.334	1613	2083	0.925	8	19093
d10r09	4.128	3643	3466	0.628	11	68052
d10r10	1.789	982	1915	1.033	13	28367
d11r01	2.970	2297	1655	0.859	9	17015
d11r02	2.308	1799	1801	0.865	12	14677
d11r03	5.700	6093	6376	0.473	9	16014
d11r04	6.514	8401	6922	0.336	23	61862
d11r05	5.952	7166	3921	0.455	17	18998
d11r06	2.607	1949	1503	0.886	9	38399
d11r07	1.639	602	1727	0.925	9	73634
d11r08	1.801	1206	723	0.957	6	4520

T Field	SS RMSE (m)	SS Phi (m^2)	Transient Phi (m^2)	Steady-State-Fit Slope	# of Failed Well Responses	Time to WIPP boundary (yr)
d11r09	2.073	858	1712	0.901	7	7199
d11r10	3.135	2363	1767	0.827	5	14358
d12r01	3.378	2921	3432	0.827	14	23936
d12r02	2.459	1795	1426	0.880	10	26919
d12r03	1.618	558	1530	0.971	11	16780
d12r04	6.182	7395	12605	0.449	20	15619
d12r05	1.522	918	1463	0.993	6	5655
d12r06	1.602	539	1271	0.958	13	39399
d12r07	2.016	945	1844	0.862	9	18283
d12r08	2.630	1879	4627	0.857	16	7981
d12r09	2.369	1671	2784	0.898	11	9414
d12r10	7.762	11431	11606	0.138	18	32059
d13r01	2.163	1061	1753	0.924	11	21032
d13r02	2.881	2054	3715	0.888	14	25639
d13r03	3.444	2580	3192	0.909	11	11493
d13r04	5.302	5856	4588	0.561	13	40601
d13r05	3.343	2671	4750	0.790	12	34247
d13r06	2.410	1441	2377	0.915	10	41400
d13r07	2.280	1395	1606	0.908	10	24211
d13r08	1.879	779	1544	0.882	9	20313
d13r09	1.919	776	1379	0.919	14	36260
d13r10	6.063	6685	2693	0.360	14	220354
d21r01	2.151	1555	2307	0.942	13	10042
d21r02	2.087	1431	2473	0.928	9	9023
d21r03	2.346	1299	744	0.907	6	11671
d21r04	2.523	1978	2908	0.905	13	15717
d21r05	2.001	932	1417	0.960	10	23750
d21r06	1.721	655	1688	0.962	8	20715
d21r07	2.182	1179	2725	0.934	9	20141
d21r08	6.620	8618	5337	0.534	14	19534
d21r09	7.750	11501	11124	0.397	19	33308
d21r10	2.959	2226	4615	0.974	13	7384
d22r01	23.126	94895	18190	0.103	15	47563
d22r02	3.629	3197	5250	0.785	10	101205
d22r03	4.061	3464	3119	0.642	11	7067
d22r04	4.894	5073	4068	1.017	12	10537
d22r05	3.566	3160	9863	0.797	18	14385
d22r06	2.469	1145	3635	0.900	9	44309
d22r07	2.080	999	1413	0.916	9	21589
d22r08	1.837	809	1681	0.914	10	30771
d22r09	1.822	724	1734	0.988	19	15870
d22r10	2.452	1684	735	1.004	5	39116

Reverse type signifies T fields not meeting final acceptance criteria discussed in Section 4.
Bold italics type signifies 100 final accepted T fields as discussed in Section 4.

All nine RMSE values greater than 20 m correspond to T fields that McKenna and Hart (2003a) did not consider to have been successfully calibrated. Figure 2 shows the RMSE values plotted against travel time, and shows that the high RMSE values tend to be associated with long travel times. For RMSE values less than approximately 6 m, travel times tend to cluster below approximately 50,000 years. Applying an RMSE cutoff value of 6 m would leave 117 T fields, with all but one having travel times less than 102,000 years (Figure 3; the outlier with a travel time of ~241,000 years, d01r06, is not shown).
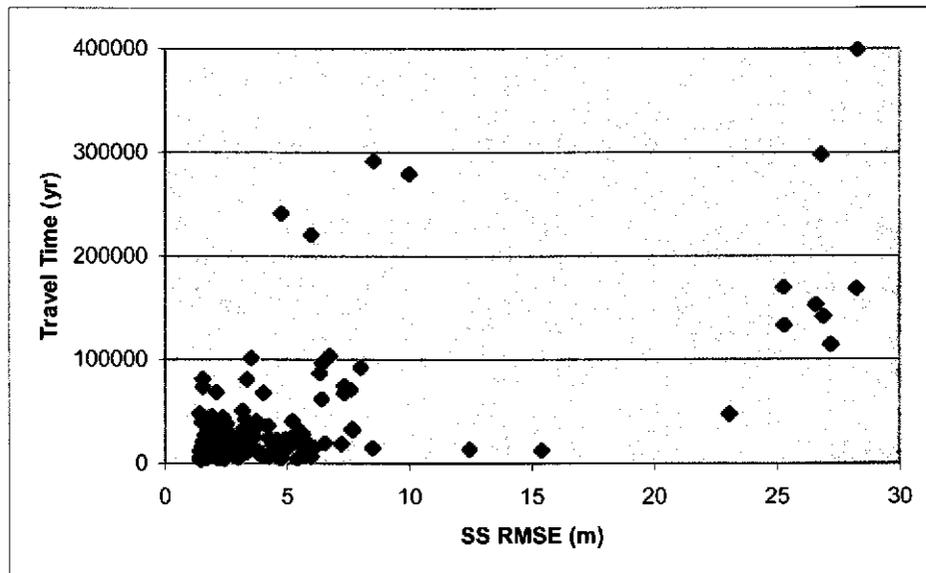
Figure 2.   Steady-state RMSE values and associated travel times.
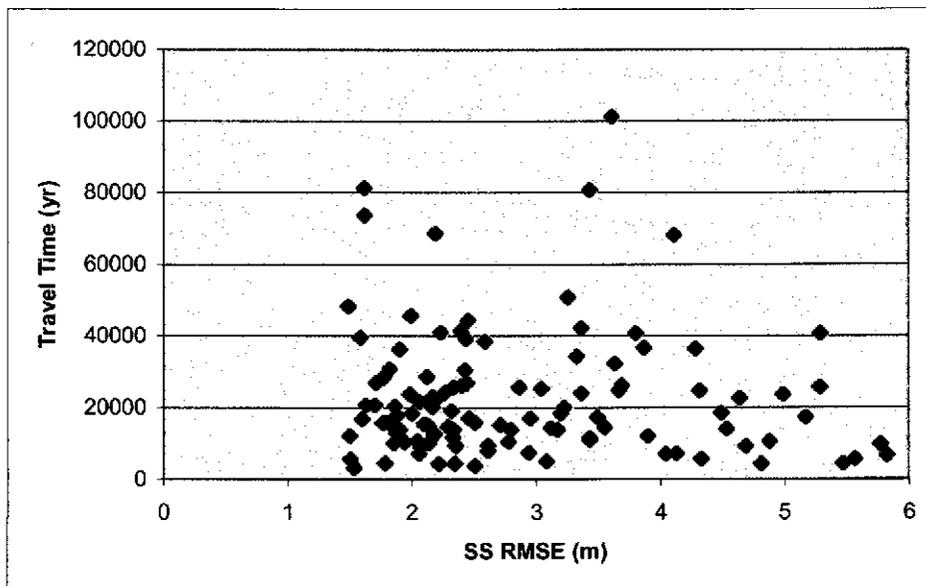
Figure 3.   Travel times for fields with steady-state RMSE <6 m.

13

3.2   Fit to Steady-State Heads

In the Excel *d##r##.xls* files, the steady-state heads are shown plotted against the modeled heads in a graph extending across columns R-X and rows 2-20 (approximately), with a unit-slope line shown as a reference. Figure 4 provides an example of such a plot for one T field. For each plot of steady-state heads, the slope of the best-fit line through all of the data except for the data for H-9b is calculated using the Excel SLOPE function (SLOPE(H2:H35,G2:G35)), with the result given in cell S22. The data for H-9b, the southernmost well, were excluded from this calculation because the southern model boundary condition consistently caused the modeled H-9b head to be significantly lower than the measured head. Inasmuch as the gradient in the extreme southern portion of the modeling domain is unimportant with respect to transport across the southern half of the WIPP site, the exclusion of the H-9b data should improve the accuracy of the slope calculation in the area of interest.
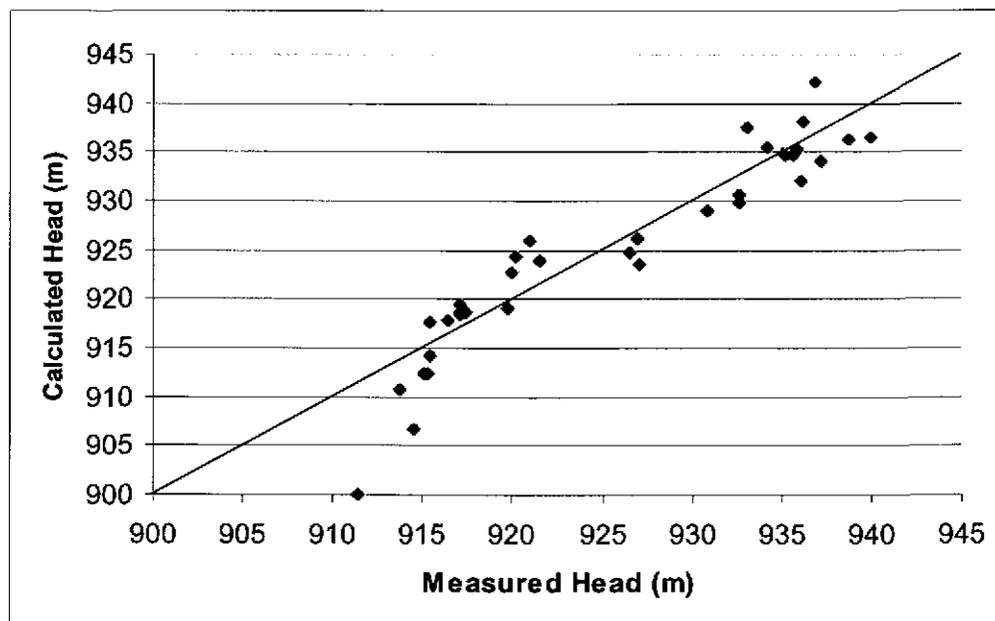
Figure 4.   Measured versus modeled steady-state heads for T field d21r10.

The slopes of the best-fit lines through the measured vs. modeled steady-state heads are tabulated in column I of file *Tfield_stats.xls* and shown plotted against travel time in Figure 5. Steady-state-fit slopes less than 0.5 appear to lead to significantly longer travel times, consistent with the low hydraulic gradients the low slopes imply. Of the 116 T fields with steady-state-fit slopes greater than 0.5, all but nine have travel times less than 50,000 years. Figure 6 shows the slopes and travel times for these 116 fields (the outlier with a travel time of ~241,000 years, d01r06, is not shown), and indicates that travel time is not sensitive to steady-state-fit slopes above 0.5.
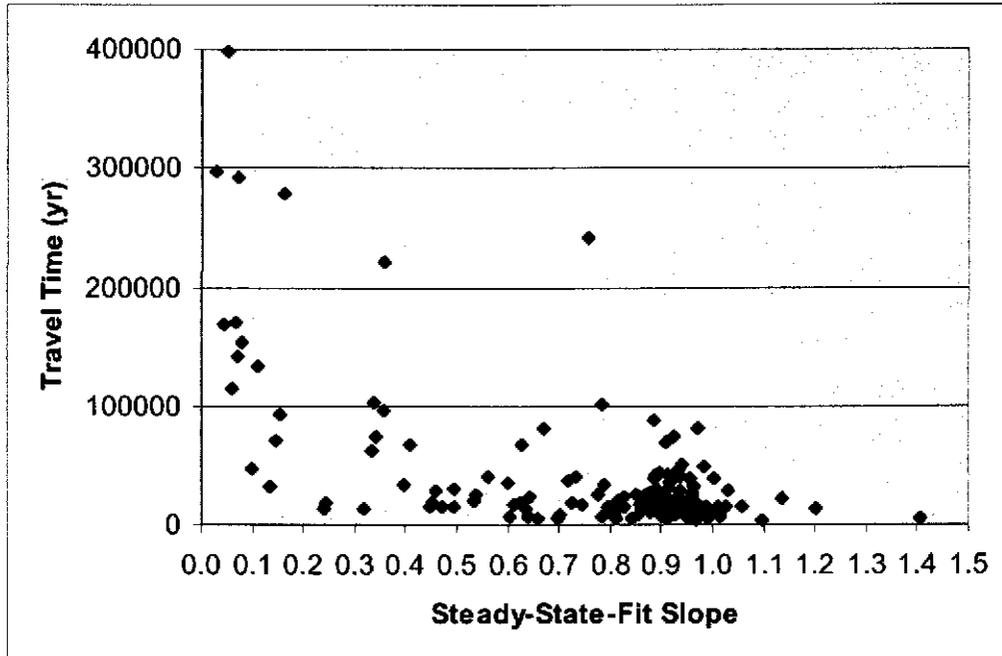
Figure 5.   Steady-state-fit slope versus travel time for all fields.
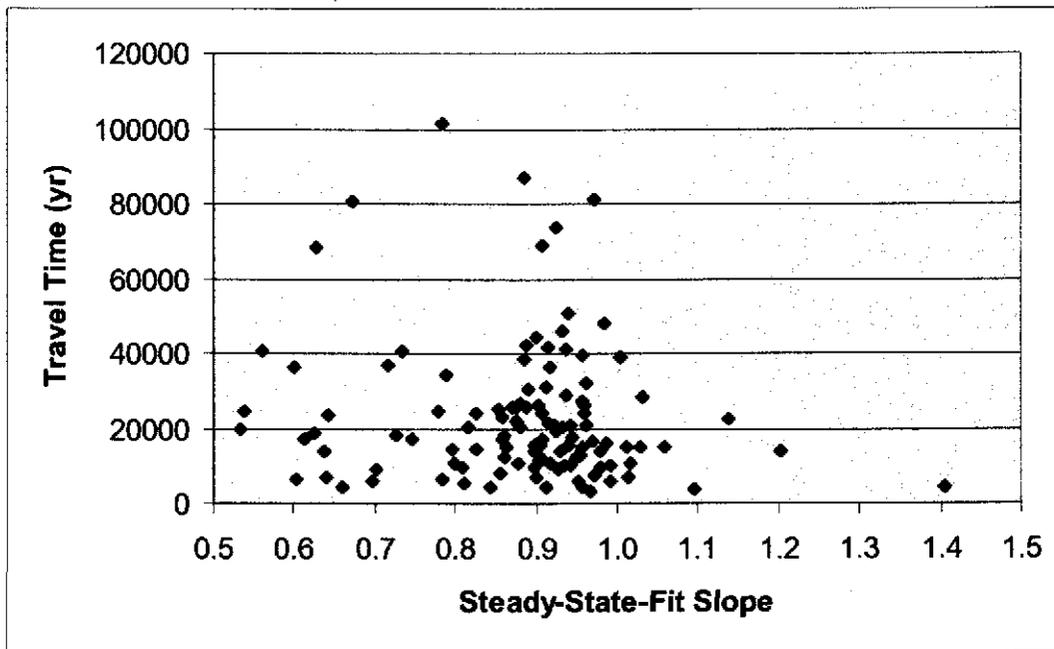
Figure 6.   Steady-state-fit slope versus travel time for slopes >0.5.

15

3.3 *Phi*

Transient phi values for all the completed T fields are calculated in cell Y25 in the ***d##r##.xls*** files, tabulated in column E in file ***Tfield_stats.xls***, and plotted against travel time in Figure 7. As phi values decrease, particularly as they get below approximately 5,000 m^2, travel times tend to cluster below approximately 50,000 years, but little correlation is seen between transient phi and travel time. Figure 8 shows transient phi versus travel time for the 123 fields with transient phi values less than 8,000 m^2, excluding the five outliers that have travel times greater than 168,000 years. This plot suggests that the degree of scatter in the travel times tends to decrease somewhat as transient phi continues to decrease, but that the range of travel times does not. Thus, transient phi does not appear to provide an effective tool for distinguishing among T fields.
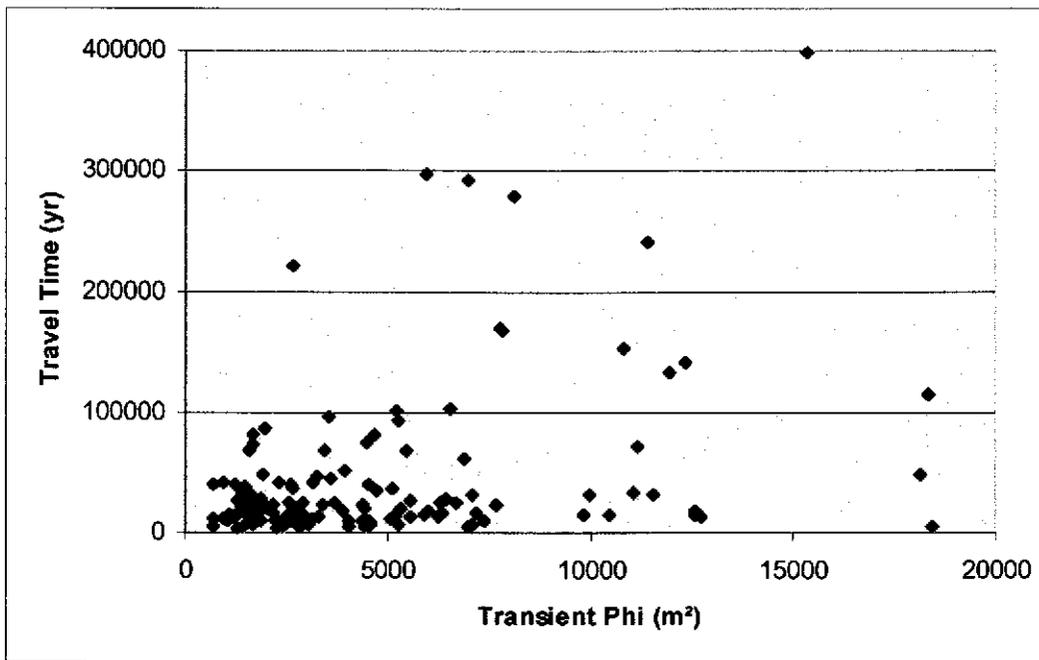
Figure 7.　　Transient phi versus travel time for all fields.

3.4 *Fit to Transient Heads*

In applying the tests described in Section 1.3 to the well responses simulated for each T field, we found that insufficient data (only six measurements) had been included for the WQSP-1 response to pumping at WQSP-2 to allow any determination of model adequacy. Thus, this response was eliminated from consideration for all T fields. Plots of the measured and modeled transient heads are shown in the ***d##r##.xls*** files discussed above, with the plots positioned to the right of the data columns for each well response. Adjacent to each plot, a PASS or FAIL grade is entered in the spreadsheet ("NULL" for WQSP2-WQSP1), generally in column Q. Figures 9 and 10 provide examples of well responses that PASS and FAIL, respectively, from T field d21r10. The numbers of responses that passed and failed are summarized in cells S27 and S28 (approximately). For the WQSP-3 responses to pumping at WQSP-1 and WQSP-2 (for which no clear drawdown was observed and "measured" values of zero were entered), the modeled response was accepted if it showed no more than 0.25 m of drawdown.
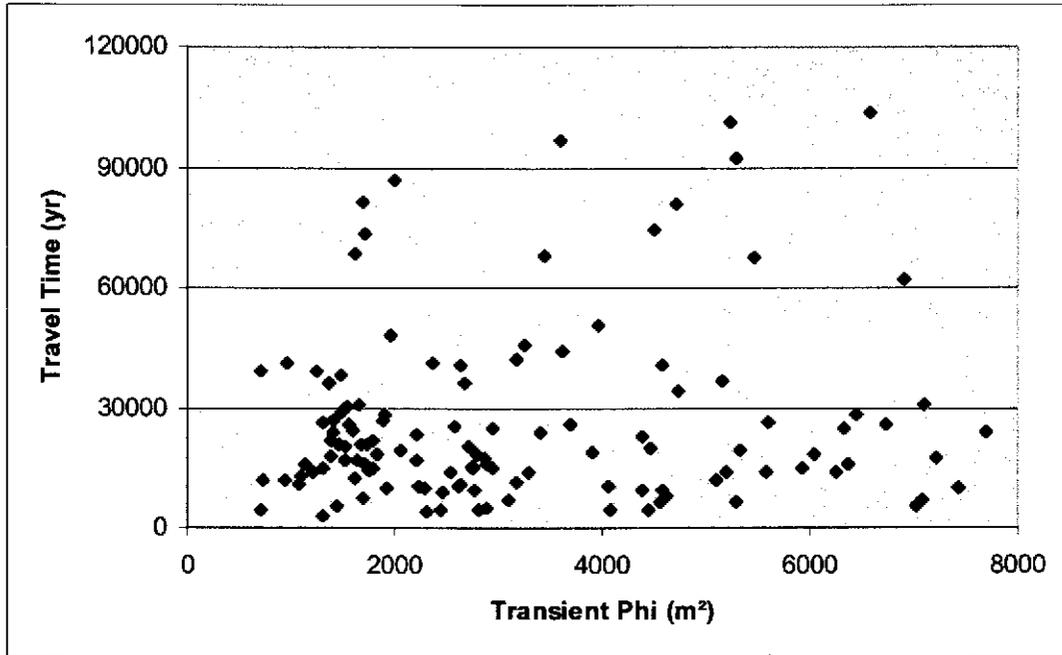
Figure 8.   Transient phi versus travel time for phi <8,000 m^2.

The number of well responses that fail the tests described in Section 1.3 should be related to the transient phi for each T field because both are measures of the match between the measured and modeled transient heads. Figure 11 shows a plot of transient phi versus the number of failed well responses for all 146 T fields. A definite correlation is evident up to a phi of approximately 8,000 m^2. Beyond that value, the number of failed well responses simply remains high ($\geq$14).

The number of failed well responses is tabulated in column F of file *Tfield_stats.xls* and plotted against travel time in Figure 12 for each of the T fields. The scatter in travel time appears to increase with 14 or more failures, but the majority of T fields still have travel times in the same range as the fields with less than 14 failures. Thus, the number of failed well responses alone does not appear to discriminate well among T fields.
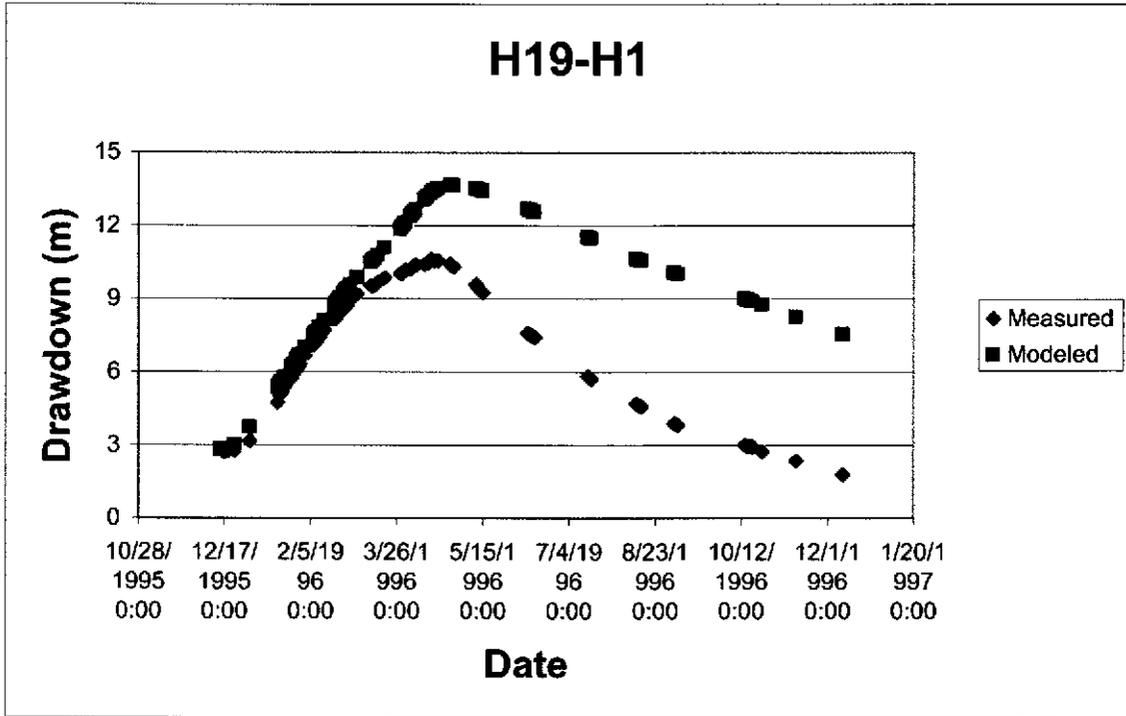
Figure 9.   Example of passing well response from T field d21r10.
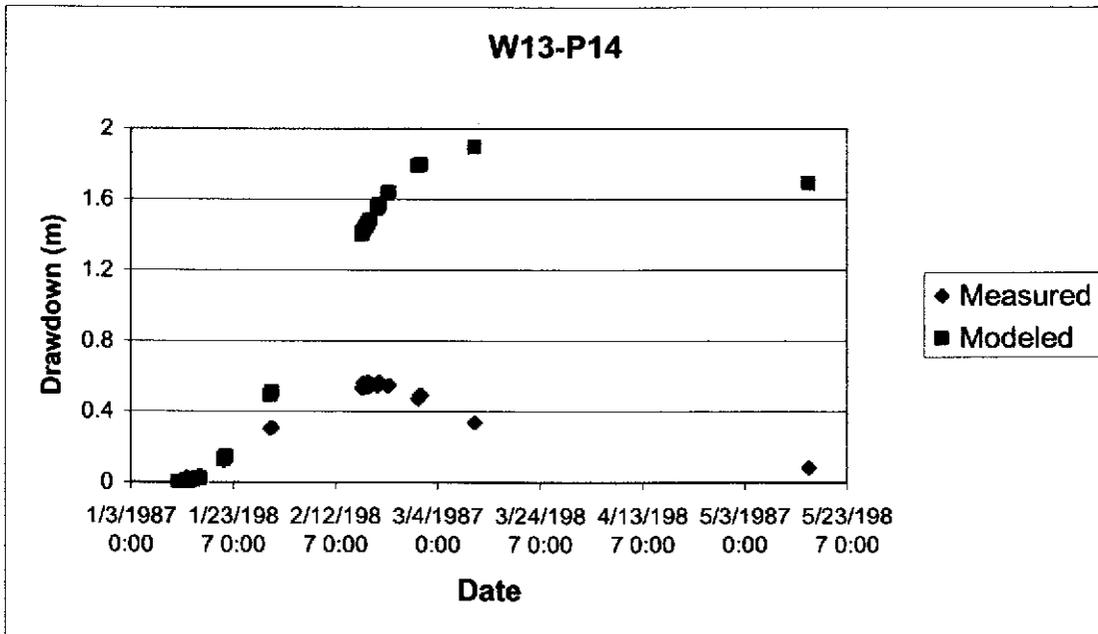
Figure 10.   Example of failing well response from T field d21r10.
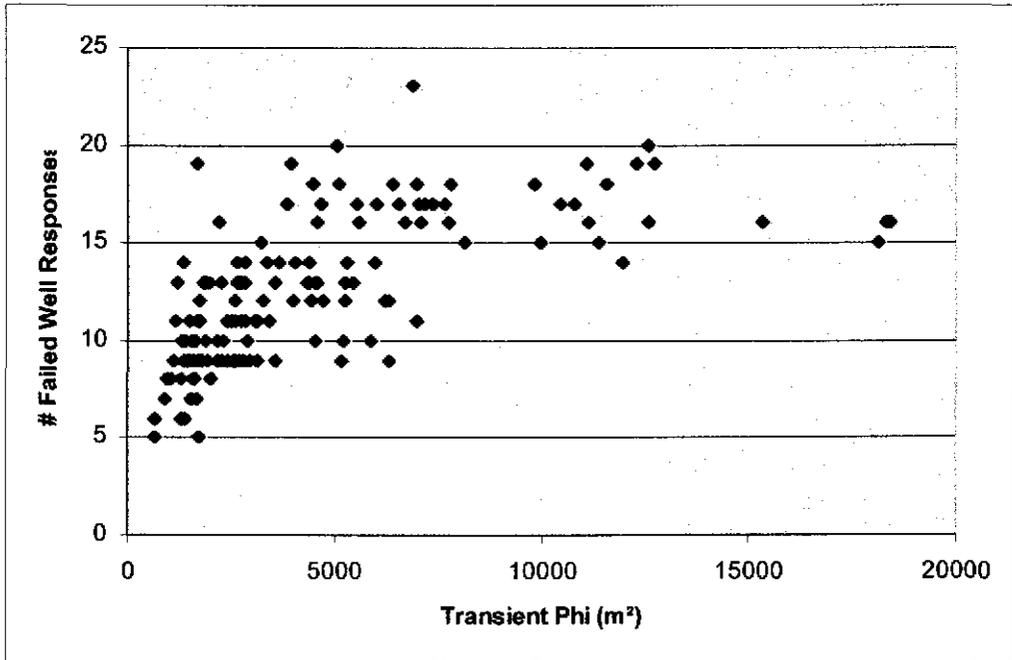
Figure 11.   Transient phi versus number of failed well responses.
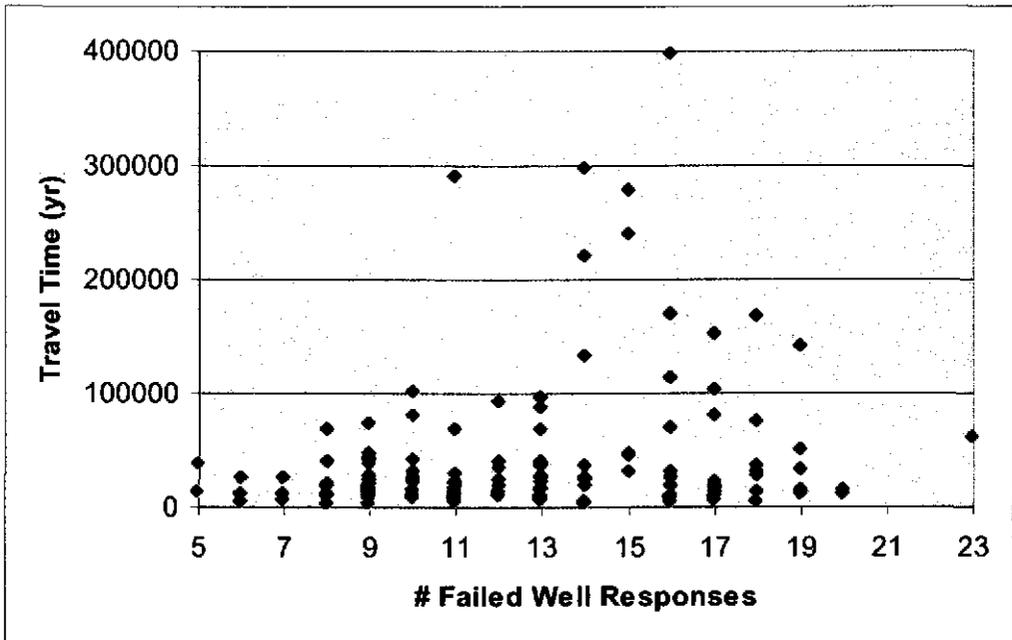
Figure 12.   Number of failed well responses versus travel time.

4. Final Acceptance Criteria

Of the criteria discussed above, the two related to the steady-state heads (RMSE and steady-state-fit slope) appear to be more effective at identifying poorly calibrated T fields than the two related to transient heads (transient phi and number of failed well responses). The range and scatter of travel times appears to increase at RMSE values beyond 6 m. Applying an RMSE cutoff of 6 m leaves 117 T fields, all with travel times less than 102,000 years except one (d01r06). This cutoff also excludes all T fields with steady-state-fit slopes less than 0.45. Steady-state-fit slopes less than approximately 0.5 appear to lead to significantly longer travel times, consistent with the low hydraulic gradients the low slopes imply. If we simply apply a cutoff of a minimum steady-state-fit slope of 0.5, we are left with 116 T fields, again with travel times less than 102,000 years (except d01r06), and also with RMSE values less than 8.6 m. Five T fields that meet the RMSE less than 6 m criterion fail the steady-state-fit slope greater than 0.5 criterion, while four T fields meeting the slope criterion fail the RMSE criterion. Thus, 112 T fields meet both criteria while 121 T fields meet at least one of the criteria.

Figure 13 shows a cumulative distribution function (CDF) for the 121 T fields meeting the RMSE and/or steady-state-fit slope criteria discussed above. Also shown are curves representing the 100 T fields with RMSE values <5 m and transient phi values <8000 m^2, and the 100 T fields with the largest steady-state-fit slopes (>0.72). All three CDF's are very similar, the most significant difference being that imposing a cutoff value on transient phi eliminates the T field with the longest travel time (d01r06). To illustrate the effects of imposing more stringent constraints on T-field acceptance, a fourth CDF is shown in Figure 13 that represents the 23 T fields that have RMSE values less than 2 m and transient phi values less than 2000 m^2. These 23 T fields all have steady-state-fit slopes greater than 0.88. This CDF generally shows travel times similar to those of the other CDF's, except at the tails of the distribution which are poorly defined because of the relatively small sample size. Thus, because all the CDF's shown are similar, all 121 T fields meeting the steady-state-fit slope or RMSE criteria are considered to be acceptably calibrated. The T fields that have been rejected are shown in reverse type in Table 1.

Because we only need 100 T fields, we can refine the criteria to eliminate more T fields. Given that lower travel times provide a conservative (in terms of leading to increased solute transport) way to discriminate among sets of T fields, the 100 T fields with RMSE values <5 m and transient phi values <8000 m^2 have been selected for use in CRA calculations of radionuclide transport through the Culebra because that set excludes the calibrated T field with the longest travel time. These T fields are highlighted in bold italicized type in Table 1.

For comparison purposes, the CDF of travel times for these 100 T fields is plotted in Figure 14 with the CDF of travel times for the 100 transient-calibrated T fields used in the CCA (Wallace, 1996). Generally speaking, travel times are two to three times as long in the CRA fields as in the CCA fields. Considering the degree of uncertainty involved in characterizing a geologic medium on the scale of the T fields, a factor of two or three difference in travel-time CDF's represents excellent agreement.
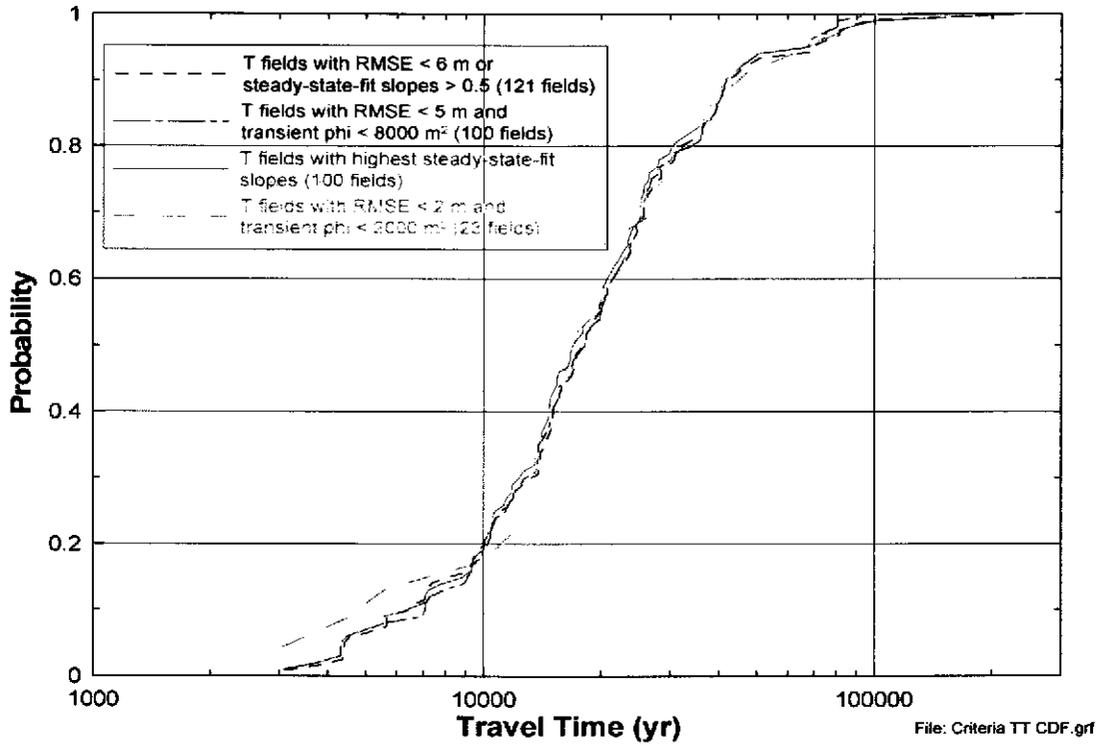
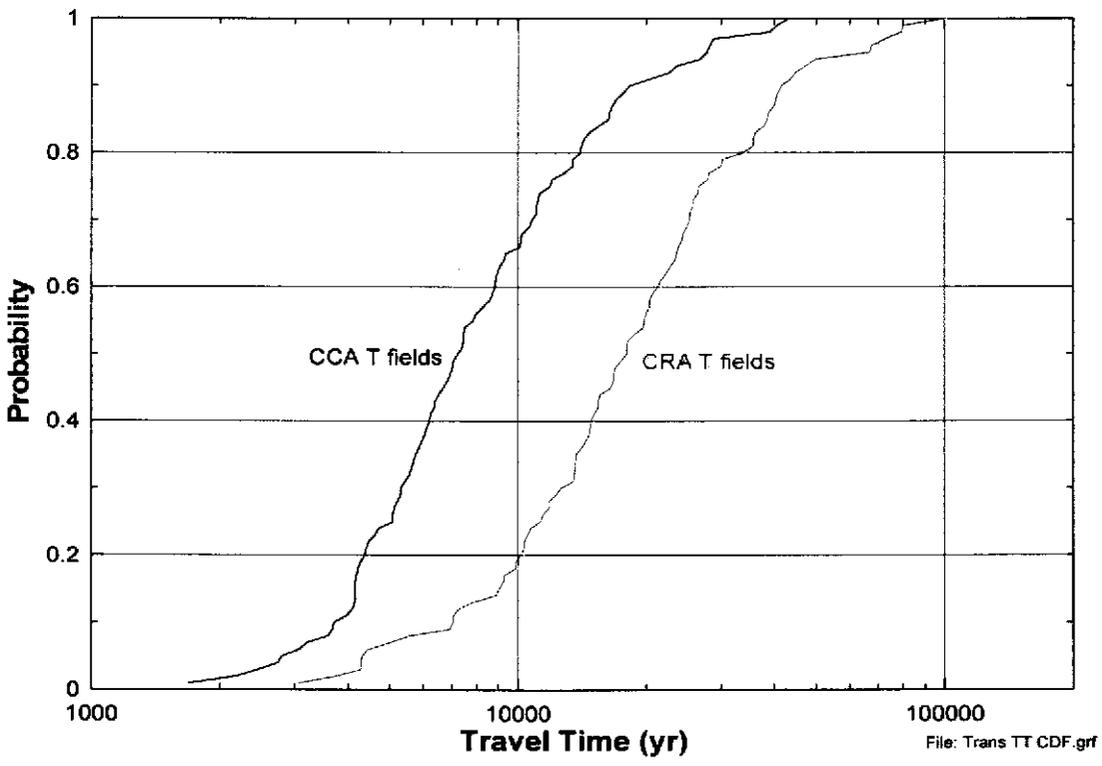Figure 13.   Travel-time CDF's for different sets of T fields.

Figure 14.   Travel-time CDF's for CCA and CRA T fields.

21

5. Software Used

All software used in the AP-100 Task 1 activities was run on Dell PC's running **Windows 2000 Professional**.

All data files were processed using **Excel 2000** from Microsoft.

Graphing was performed using **Excel 2000** and **Grapher 3.03** (commercial, off-the-shelf software) from Golden Software, Inc.

Pumping-test simulations were run using **nSIGHTS 1.0**.

6.   Listing of Computer Files

All computer files are available both on CD and on the CMS library @ LIBTFIELDS.

File name	Source	Contents
d##r##_transient.res	McKenna and Hart (2003a)	PEST residuals files (146) with measured and modeled heads, residuals, and other information for each calibrated T field
d##r##.xls	created	Excel files (146) containing data from *d##r##_transient.res* files and showing: graphs of measured and modeled heads; calculations of phi, RMSE, and steady-state-fit slope; and assignment of PASS/FAIL rating to modeled well responses and summation of grades.
Tfield_stats.xls	created	Excel file summarizing and graphing T-field information (phi, RMSE, steady-state-fit slope, number of failed well responses, etc.) from all *d##r##.xls* files and travel-time information from McKenna and Hart (2003a).
T and S Variations.nPre	created	nSIGHTS file for calculation of responses shown in Appendix A
T and S Variations.nPost	output	nSIGHTS output file with simulation results

7. References

Beauheim, R.L. 2002a. "Analysis Plan for the Evaluation of the Effects of Head Changes on Calibration of Culebra Transmissivity Fields, AP-088, Revision 1." ERMS# 524785. Carlsbad, NM: Sandia National Laboratories, WIPP Records Center.

Beauheim, R.L. 2002b. Routine Calculations Report In Support of Task 3 of AP-088, Calculation of Culebra Freshwater Heads in 1980, 1990, and 2000 for Use in T-Field Calibration. ERMS# 522580. Carlsbad, NM: Sandia National Laboratories, WIPP Records Center.

Beauheim, R.L. 2003. Records Package for AP-088 Task 4, Conditioning of Base T Fields to Transient Heads: Compilation and Reduction of Transient Head Data. ERMS# 527572. Carlsbad, NM: Sandia National Laboratories, WIPP Records Center.

Corbet, T.F., and P.M. Knupp. 1996. *The Role of Regional Groundwater Flow in the Hydrogeology of the Culebra Member of the Rustler Formation at the Waste Isolation Pilot Plant (WIPP), Southeastern New Mexico*. SAND96-2133. Albuquerque, NM: Sandia National Laboratories.

Doherty, J. 2002. *Manual for PEST; 5th Edition*. Watermark Numerical Computing, Australia.

Harbaugh, A.W., E.R. Banta, M.C. Hill, and M.G. McDonald. 2000. *MODFLOW-2000, the U.S. Geological Survey Modular Ground-Water Model -- User Guide to Modularization Concepts and the Ground-Water Flow Process*. U.S. Geological Survey Open-File Report 00-92, 121 p.

Helton, J.C., J.E. Bean, J.W. Berglund, F.J. Davis, K. Economy, J.W. Garner, J.D. Johnson, R.J. MacKinnon, J. Miller, D.G. O'Brien, J.L. Ramsey, J.D. Schreiber, A. Shinta, L.N. Smith, D.M. Stoelzel, C. Stockman, and P. Vaughn. 1998. *Uncertainty and Sensitivity Analysis Results Obtained in the 1996 Performance Assessment for the Waste Isolation Pilot Plant*. SAND98-0365. Albuquerque, NM: Sandia National Laboratories.

Helton, J.C., and M.G. Marietta (editors). 2000. The 1996 Performance Assessment for the Waste Isolation Pilot Plant, Special Issue of: *Reliability Engineering and System Safety*, Vol 69, No. 1-3.

Holt, R.M., and L. Yarbrough. 2003. Addendum 2 to Analysis Report, Task 2 of AP-088, Estimating Base Transmissivity Fields. ERMS# 529416. Carlsbad, NM: Sandia National Laboratories, WIPP Records Center.

LaVenue, A.M., and B.S. RamaRao. 1992. *A Modeling Approach to Address Spatial Variability within the Culebra Dolomite Transmissivity Field*. SAND92-7306. Albuquerque, NM: Sandia National Laboratories.

Leigh, C., R. Beauheim, and J. Kanney. 2003. "Analysis Plan for Calculations of Culebra Flow and Transport: Compliance Recertification Application, AP-100." ERMS# 530172. Carlsbad, NM: Sandia National Laboratories, WIPP Records Center.

McKenna, S.A., and D.B. Hart. 2003a. Analysis Report, Task 4 of AP-088, Conditioning of Base T Fields to Transient Heads. ERMS# 531124. Carlsbad, NM: Sandia National Laboratories, WIPP Records Center.

McKenna, S.A., and D.B. Hart. 2003b. Analysis Report, Task 3 of AP-088, Conditioning of Base T Fields to Steady-State Heads. ERMS# 529633. Carlsbad, NM: Sandia National Laboratories, WIPP Records Center.

Roberts, R.M. 2002. nSIGHTS User Manual, Document Version 1.0. ERMS# 522061. Carlsbad, NM: Sandia National Laboratories, WIPP Records Center.

Rudeen, D.K. 2003. User's Manual for DTRKMF Version 1.00. ERMS# 523246. Carlsbad, NM: Sandia National Laboratories, WIPP Records Center.

U.S. Department of Energy. 1996. *Title 40 CFR Part 191 Compliance Certification Application for the Waste Isolation Pilot Plant.* DOE/CAO-1996-2184. Carlsbad, NM: U.S. DOE, Carlsbad Area Office.

Wallace, M. 1996. Records Package for Screening Effort NS11: Subsidence Associated with Mining Inside or Outside the Controlled Area. ERMS# 412918. Carlsbad, NM: Sandia National Laboratories, WIPP Records Center.

Appendix A

Effects of Changes in T and S on Drawdown Peak Height and Timing

To evaluate the effects that one-half order of magnitude changes in transmissivity (T) and storativity (S) might have on the timing and height of drawdown peaks at observation wells, a series of simulations was conducted using the well-test-simulator code nSIGHTS (Roberts, 2002). Base-case simulations were performed by calculating the responses that would be observed in observation wells 1 km, 2 km, and/or 3 km from a well pumping at 0.63 L/s (10 gallons per minute) for 5, 25, and/or 50 days in a medium with a T of 1×10^{-5} m^2/s and an S of 1×10^{-5}. Variations were simulated using T values of 3×10^{-6} and 3×10^{-5} m^2/s and S values of 3×10^{-6} and 3×10^{-5}. The simulations are shown in Figures A-1 through A-16. The results of these simulations are listed in Tables A-1 through A-3 in terms of the effect that the variation in T and/or S had on the height of the drawdown peak and the time at which it occurred relative to the peak in the base-case simulation.

Table A-1. Effects of T and S Variations on Drawdown Peaks 1 km from Pumping Well.

Pumping Duration		$T = 3 \times 10^{-6}$ m^2/s	$T = 1 \times 10^{-5}$ m^2/s	$T = 3 \times 10^{-5}$ m^2/s
5 days	$S = 3 \times 10^{-6}$	H: 3.33 PT: identical	H: 2.38 PT: 0.81	H: 1.36 PT: 0.78
5 days	$S = 1 \times 10^{-5}$	H: 1.08 PT: 2.01	Base Case	H: 0.75 PT: 0.82
25 days		H: 1.56 PT: 1.13		H: 0.53 PT: 0.98
50 days		H: 1.83 PT: 1.05		H: 0.48 PT: 0.99
5 days	$S = 3 \times 10^{-5}$	H: 0.36 PT: 4.89	H: 0.36 PT: 1.82	H: 0.33 PT: identical

H: ratio of peak height to base-case peak height
PT: ratio of time of peak occurrence relative to time of base-case peak

Table A-2. Effects of T and S Variations on Drawdown Peaks 2 km from Pumping Well.

Pumping Duration		$T = 3 \times 10^{-6}$ m^2/s	$T = 1 \times 10^{-5}$ m^2/s	$T = 3 \times 10^{-5}$ m^2/s
5 days	$S = 3 \times 10^{-6}$	H: 3.33 PT: identical	H: 3.14 PT: 0.47	H: 2.44 PT: 0.36
5 days	$S = 1 \times 10^{-5}$	H: 1.004 PT: 2.78	Base Case	H: 0.95 PT: 0.48
5 days	$S = 3 \times 10^{-5}$	H: 0.33 PT: 7.98	H: 0.33 PT: 2.59	H: 0.33 PT: identical

H: ratio of peak height to base-case peak height
PT: ratio of time of peak occurrence relative to time of base-case peak

Table A-3. Effects of T and S Variations on Drawdown Peaks 3 km from Pumping Well.

Pumping Duration		$T = 3 \times 10^{-6}$ m²/s	$T = 1 \times 10^{-5}$ m²/s	$T = 3 \times 10^{-5}$ m²/s
5 days	$S = 3 \times 10^{-6}$	H: 3.33 PT: identical	H: 3.30 PT: 0.38	H: 3.00 PT: 0.22
5 days	$S = 1 \times 10^{-5}$	H: 0.999 PT: 3.23	Base Case	H: 0.99 PT: 0.40
25 days		H: 1.03 PT: 2.34		H: 0.85 PT: 0.67
50 days		H: 1.10 PT: 1.87		H: 0.73 PT: 0.83
5 days	$S = 3 \times 10^{-5}$	H: 0.33 PT: 9.64	H: 0.33 PT: 2.97	H: 0.33 PT: identical

H: ratio of peak height to base-case peak height
PT: ratio of time of peak occurrence relative to time of base-case peak

The simulations show that if the modeled T value is lower than the actual T value, too much drawdown will be simulated (with the difference increasing with pumping time and decreasing with distance) and the maximum drawdown will occur later than was observed. If the modeled T value is higher than the actual T value, too little drawdown will be simulated (again, the difference increases with pumping time and decreases with distance) and the maximum drawdown will occur sooner than was observed. If the modeled S value is lower than the actual S value, too much drawdown will be simulated (with the difference increasing with distance) and the maximum drawdown will occur sooner than was observed. If the modeled S value is higher than the actual S value, too little drawdown will be simulated and the maximum drawdown will occur later than was observed. Parallel changes in T and S (i.e., keeping hydraulic diffusivity (T/S) constant) alter the amount of drawdown simulated (more if T and S are decreased, less if T and S are increased) but do not affect the time at which the maximum drawdown occurs. Opposing changes in T and S increase the difference in the time at which peak drawdown occurs (significantly when T is decreased and S increased, see Figures A-10 and A-14) but decrease (or do not affect) the difference between measured and modeled maximum drawdown relative to the case in which only S is changed.

In general terms, changes in S cause the magnitude of drawdown to change by as much as the inverse of the change in S. That is, an increase in S of a factor of three will cause a decrease in drawdown of at most a factor of three. More of the possible change is observed as distance from the pumping well increases. Similarly, the magnitude of drawdown is inversely proportional to T. But while a threefold increase in T might (depending on wellbore storage and skin) cause a threefold decrease in drawdown at the pumping well, this effect dissipates with distance.

For the specific case of factor-of-three changes in T and S and observation wells one or more km distant from the pumping well, the results can be summarized as follows:

- If the modeled peak occurs early and high (relative to the measured peak), S is too low and the maximum modeled drawdown can be up to three times greater than the maximum measured drawdown.
- If the modeled peak occurs early and low, T is too high and the maximum modeled drawdown can be up to two times lower than the maximum measured drawdown.
- If the modeled peak occurs late and high, T is too low and the maximum modeled drawdown can be up to two times higher than the maximum measured drawdown.
- If the modeled peak occurs late and low, S is too high and the maximum modeled drawdown can be up to three times lower than the maximum measured drawdown.
- If the modeled peak occurs at the same time as the measured peak but is high, the diffusivity (T/S) is correct, but both T and S are too low and the maximum modeled drawdown can be up to three times greater than the maximum measured drawdown.
- If the modeled peak occurs at the same time as the measured peak but is low, the diffusivity (T/S) is correct, but both T and S are too high and the maximum modeled drawdown can be up to three times lower than the maximum measured drawdown.

No quantitative criteria were established for how much earlier or later modeled peaks could occur relative to measured peaks because of the wide range observed in these calculations (calculated peaks occurring a factor of five sooner to a factor of ten later than the observed peaks) and because of the variability in pumping durations and distances to observation wells associated with the measured responses.
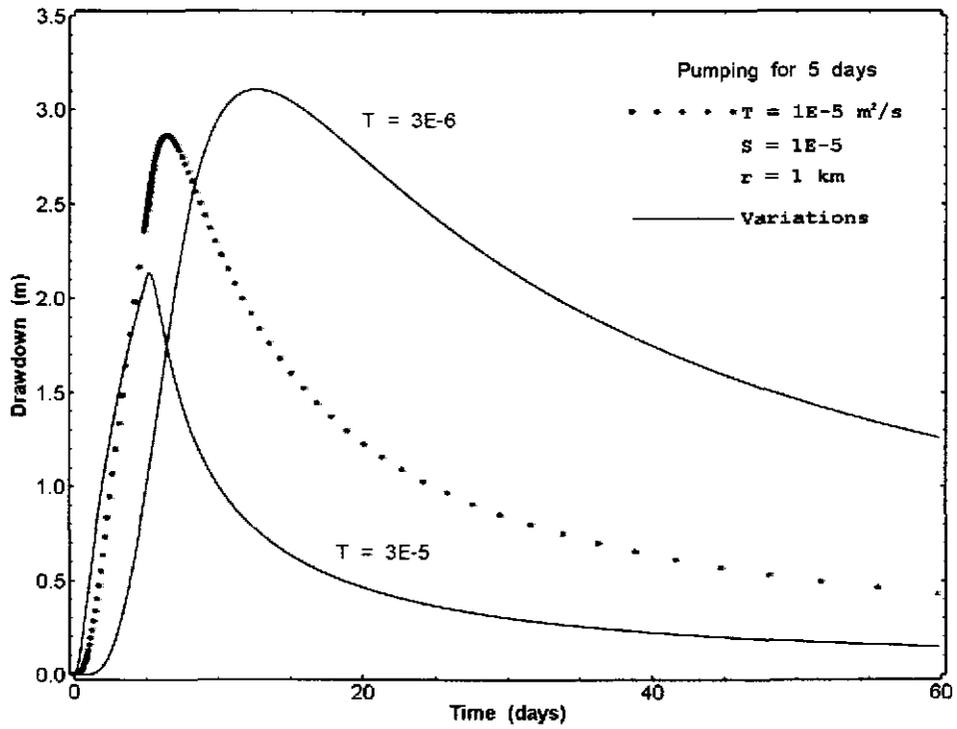
Figure A-1. Effect on drawdown at 1 km of changing T, pumping for 5 days.
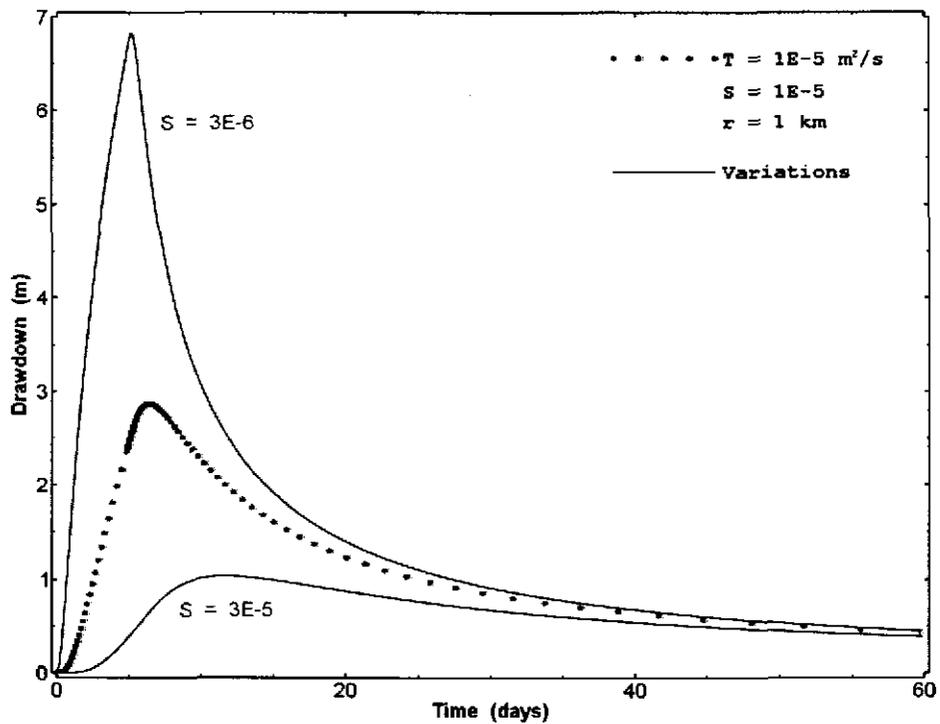
Figure A-2. Effect on drawdown at 1 km of changing S, pumping for 5 days.

30
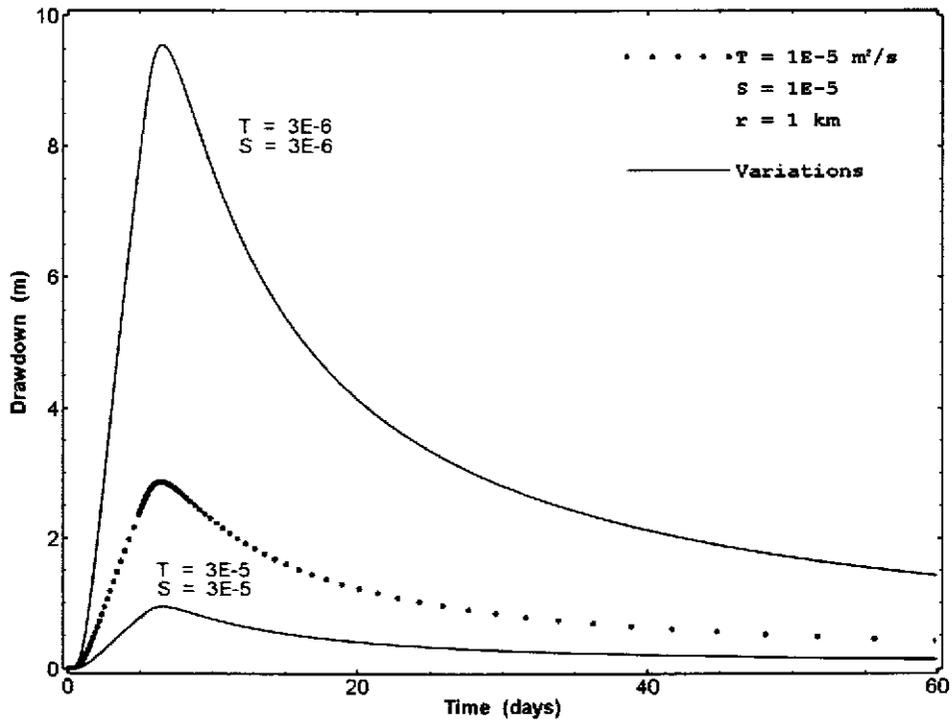
Figure A-3. Effect on drawdown at 1 km of changing T and S together, pumping for 5 days.
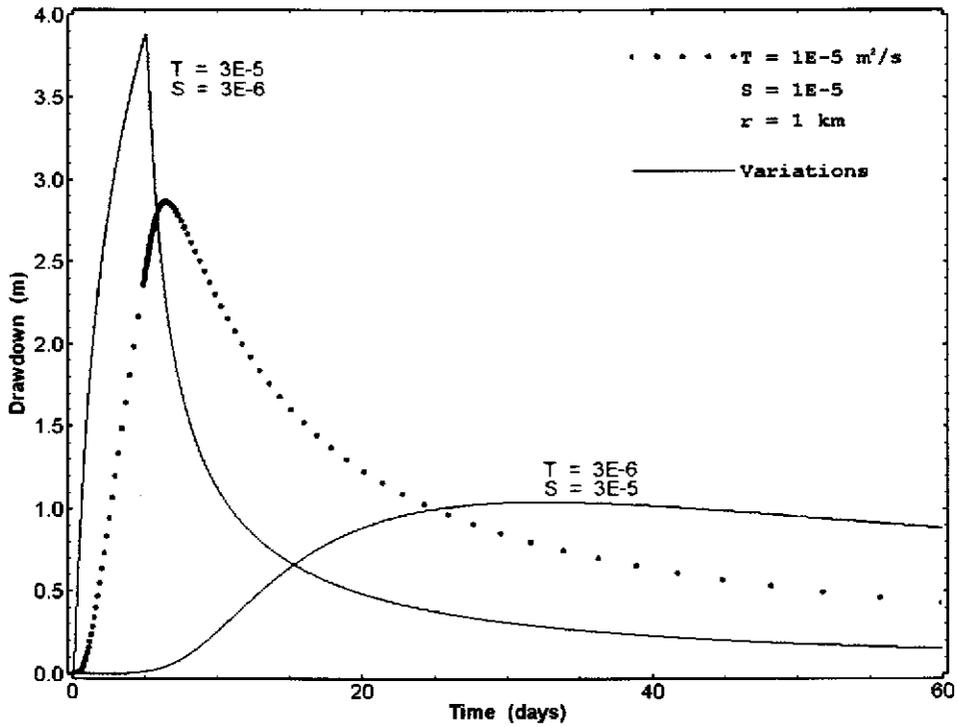
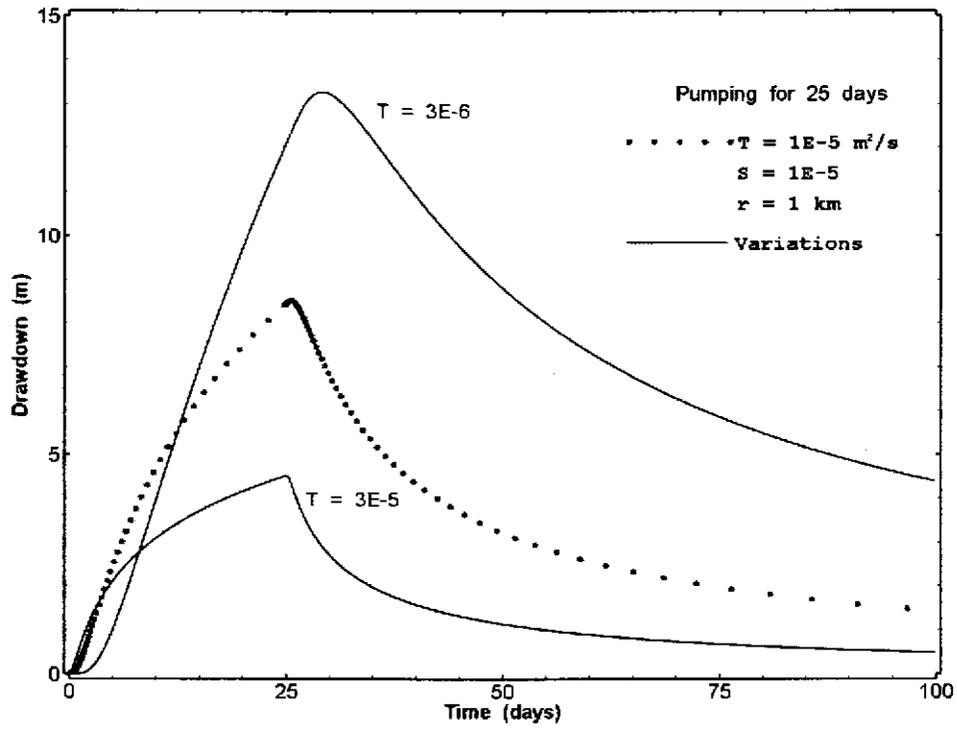Figure A-4. Effect on drawdown at 1 km of changing T and S oppositely, pumping for 5 days.

31

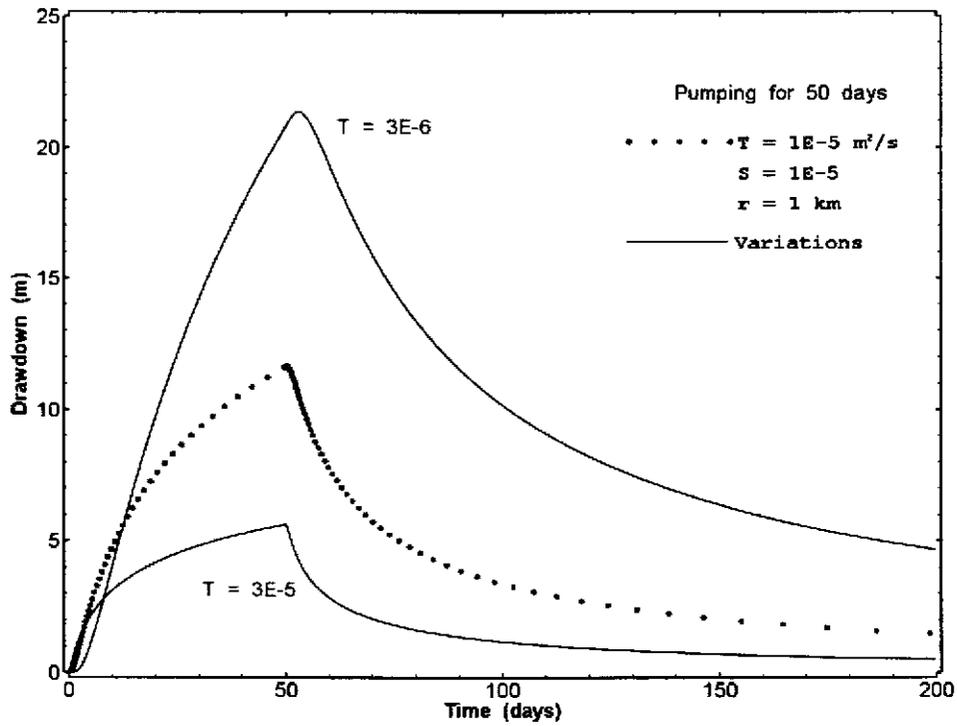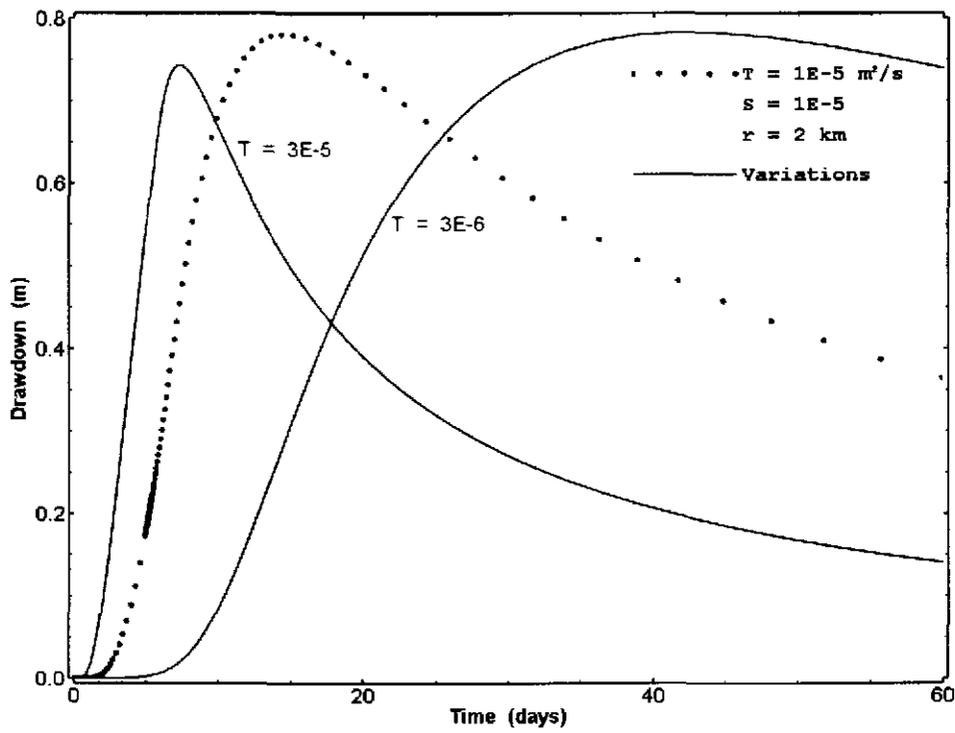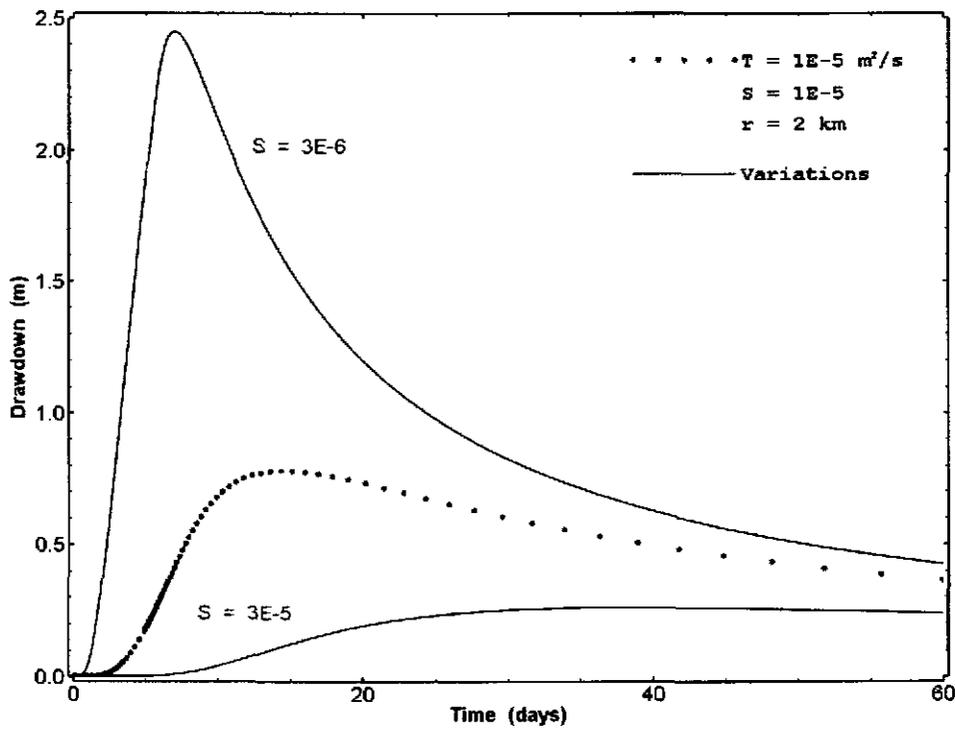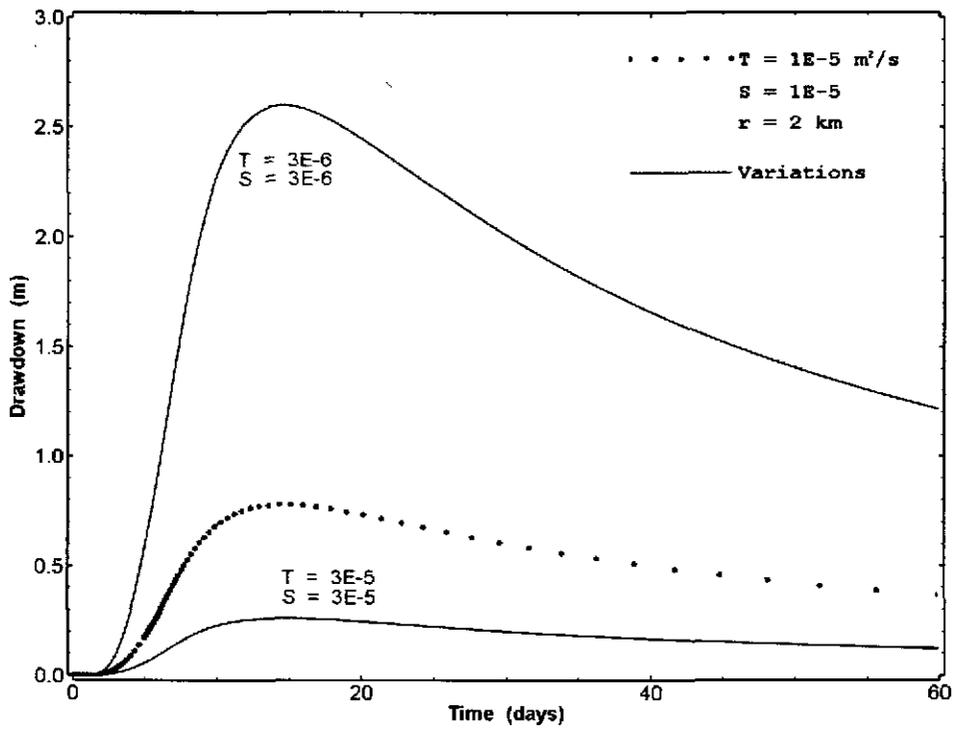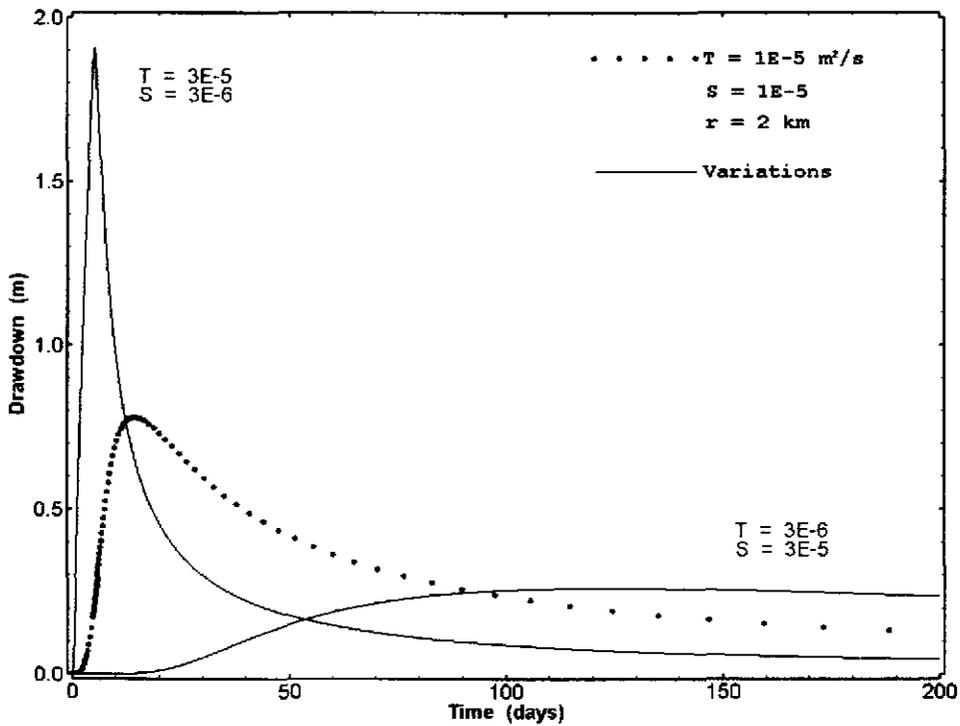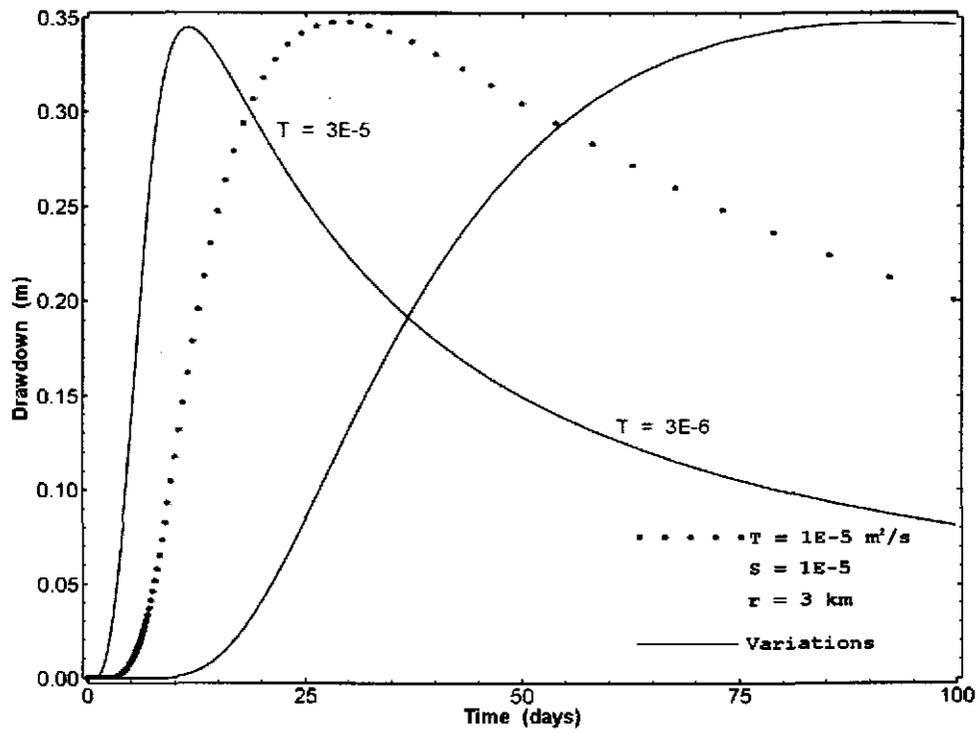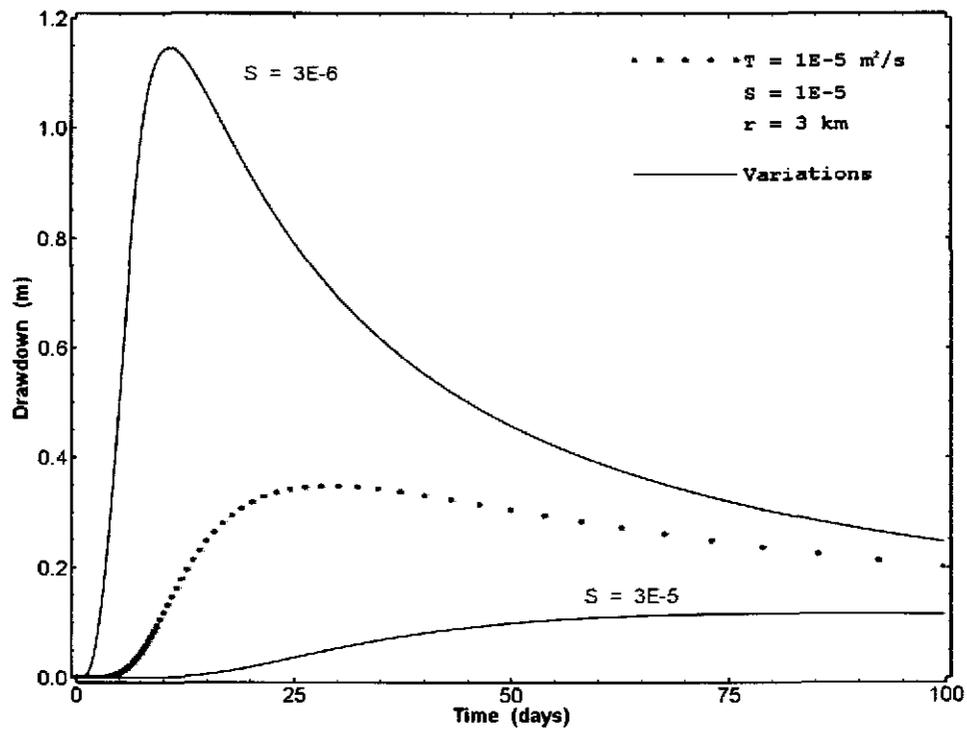Figure A-5. Effect on drawdown at 1 km of changing T, pumping for 25 days.

Figure A-6. Effect on drawdown at 1 km of changing T, pumping for 50 days.

32

Figure A-7. Effect on drawdown at 2 km of changing T, pumping for 5 days.

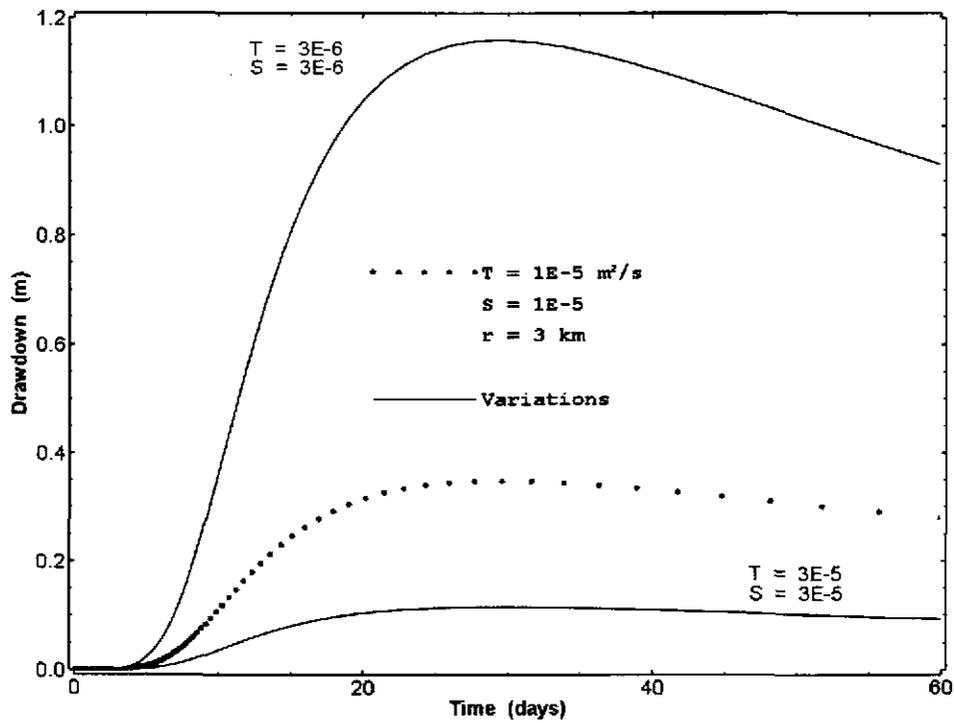Figure A-8. Effect on drawdown at 2 km of changing S, pumping for 5 days.

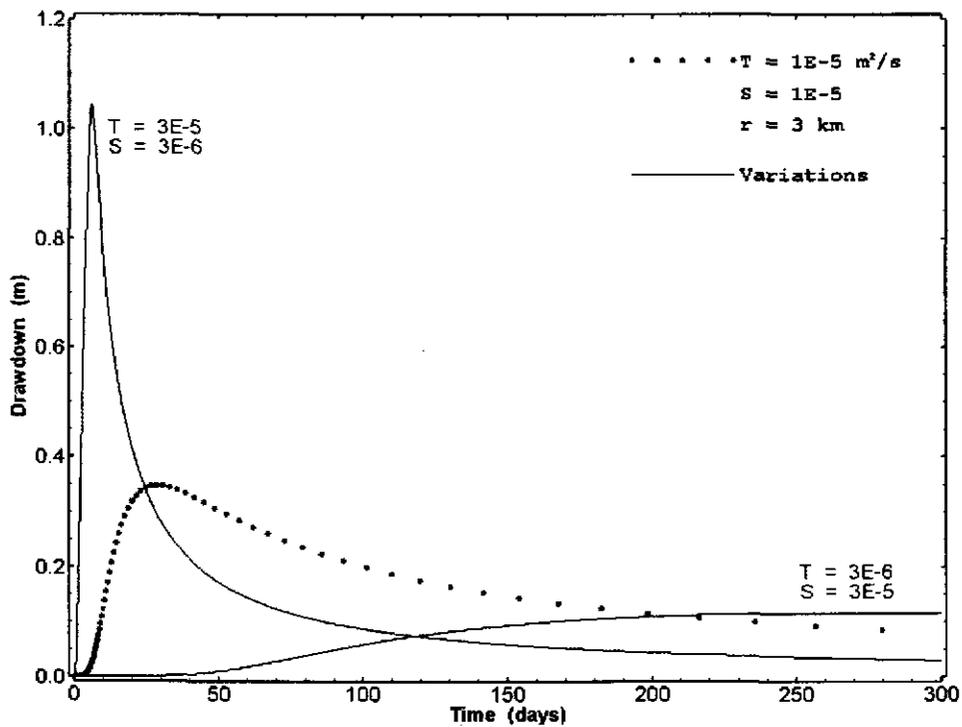Figure A-9. Effect on drawdown at 2 km of changing T and S together, pumping for 5 days.

Figure A-10. Effect on drawdown at 2 km of changing T and S oppositely, pumping for 5 days.

34

Figure A-11. Effect on drawdown at 3 km of changing T, pumping for 5 days.

Figure A-12. Effect on drawdown at 3 km of changing S, pumping for 5 days.

35

Figure A-13. Effect on drawdown at 3 km of changing T and S together, pumping for 5 days.

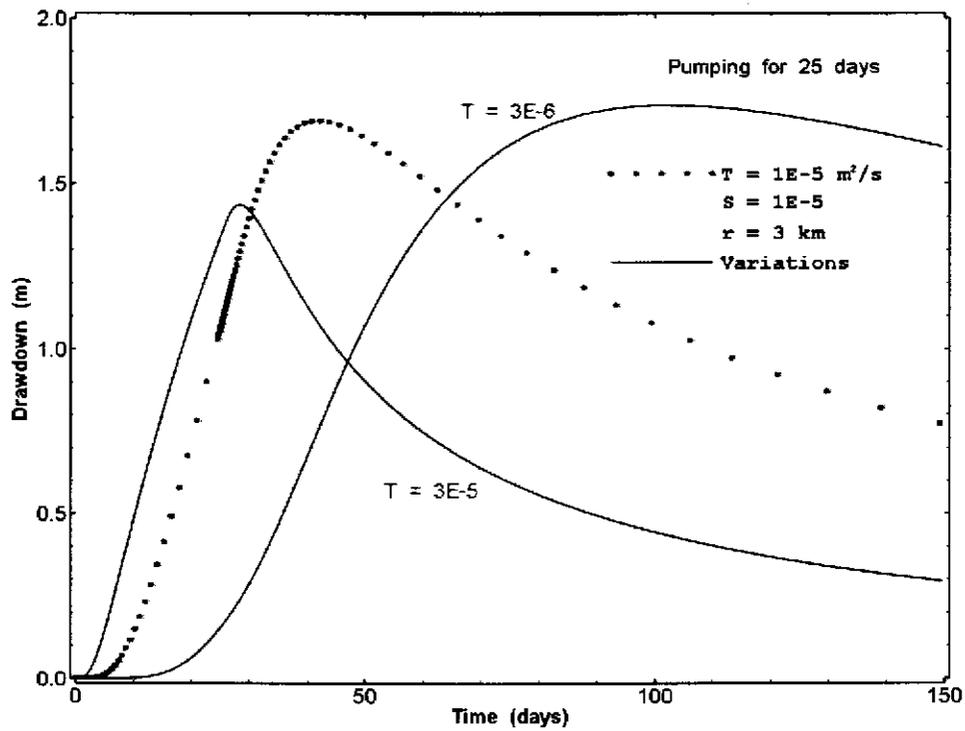Figure A-14. Effect on drawdown at 3 km of changing T and S oppositely, pumping for 5 days.

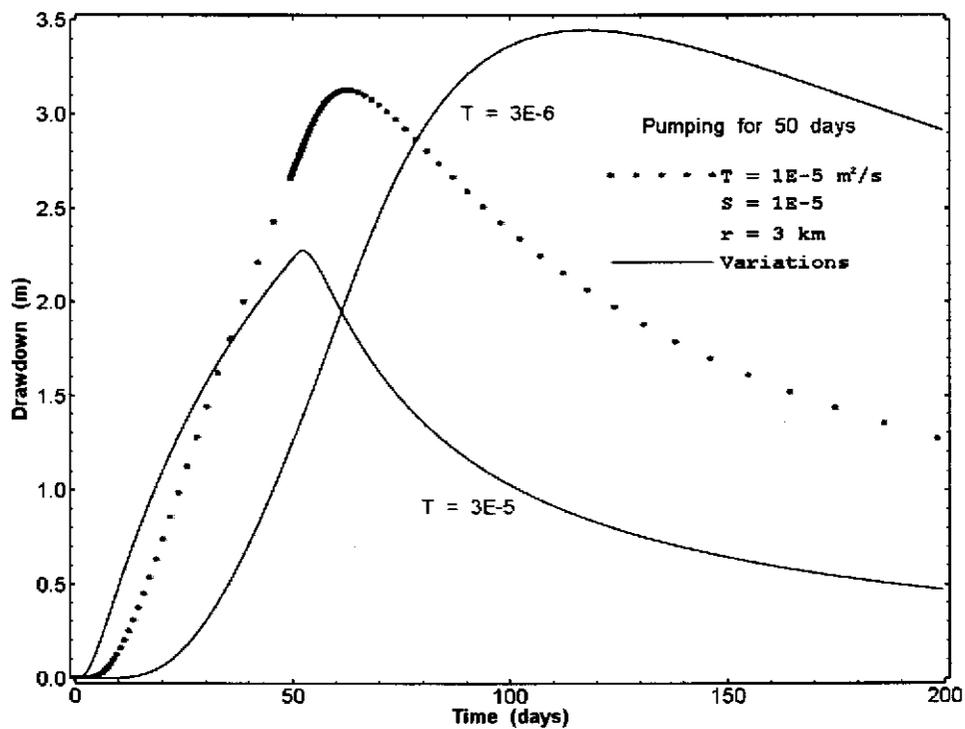Figure A-15. Effect on drawdown at 3 km of changing T, pumping for 25 days.

Figure A-16. Effect on drawdown at 3 km of changing T, pumping for 50 days.